

# **Indigenous Fabrication and Characterization of Ceramic Composite Ballistic Armour**



**By  
Muhammad Shahid Bashir**

**School of Chemical and Materials Engineering  
National University of Sciences and Technology  
2022**

# **Indigenous Fabrication and Characterization of Ceramic Composite Ballistic Armour**



Muhammad Shahid Bashir

Reg No: 00000276302

**This thesis is submitted as a partial fulfillment of the requirements  
for the degree of**

**MS in Materials and Surface Engineering**

**Supervisor Name: Dr. Malik Adeel Umer**

**School of Chemical and Materials Engineering (SCME)**

**National University of Sciences and Technology (NUST)**

**H-12 Islamabad, Pakistan**

**August, 2022**

## **Declaration**

I certify that this research work titled “*Indigenous Fabrication and Characterization of Composite Ballistic Armour*” is my own work. The work has not been presented elsewhere for assessment. The material that has been used from other sources has been properly acknowledged / referred.

Signature of Student

**Muhammad Shahid Bashir**

FALL2018-MS, MSE-00000276302

## **Plagiarism Certificate (Turnitin Report)**

This thesis has been checked for Plagiarism. Turnitin report endorsed by Supervisor is attached.

Signature of Student

**Muhammad Shahid Bashir**

Registration Number

FALL2018-MS, MSE-00000276302

Signature of Supervisor

## **Dedication**

*Dedicated to my teachers, parents, wife and kids*

## **Acknowledgements**

First of all, I am thankful to my Creator Allah Almighty who guided me throughout this work at every phase.

I would also like to express special thanks to my supervisor Dr. Malik Adeel Umer for his continuous help, expert guidance and strong support throughout my thesis. I would also like to pay special thanks to Brigadier Dr. Syed Waheed Ul Haq for his tremendous support and cooperation during experimentation.

Finally, I would like to express my gratitude to all the individuals who have rendered valuable assistance to my study.

## Abstract

In this research work, Al<sub>2</sub>O<sub>3</sub> based ballistic ceramic tiles were manufactured indigenously using locally available resources. Performance measurements and analysis of genuine armour were conducted to analyze their properties by using Scanning electron microscope (SEM), X-Ray Diffraction (XRD) and laser spectroscopy. Lab scale samples were fabricated using different compositions of three additives i.e TiO<sub>2</sub>, SiO<sub>2</sub> and MgO in alumina at three different sintering temperatures. High value of Young's modulus, compressive strength and hardness were achieved for the sample that incorporate the composition MgO and TiO<sub>2</sub> in alumina at the temperature >1600°C. The ballistic response of composite armour was determined against 7.62x51 mm armour projectile having a velocity of 800m/s on the optimized sample. To perform field test, the fabricated Al<sub>2</sub>O<sub>3</sub> tiles were impregnated on top of a UHMWPE panel using structural epoxy. No other layer was applied, allowing the entire momentum/impact of the projectile to fall on the ceramic tile. Ballistic tests were performed on the composite samples according to the National Institute of Justice, NIJ, level III. The performance of bare ceramic tiles having different thicknesses was evaluated by live firing and the videos of impacts were also recorded through a high-speed camera. They successfully stopped incoming projectiles by crushing the bullet and the trauma on the backing plate was observed in the allowable range.

**Key Words:** *Indigenously Fabricated Ceramic Tiles, Armour Projectile, Ballistic Response, UHMWPE panel, Alumina*

# Table of Contents

<b>Abstract.....</b>	<b>iii</b>
<b>Table of Contents.....</b>	<b>iv</b>
<b>List of Figures.....</b>	<b>vi</b>
<b>List of Tables.....</b>	<b>x</b>
<b>Chapter 1: Introduction.....</b>	<b>1</b>
1.1 Background.....	1
1.2 Literature Review .....	4
1.3 Problem Statement.....	9
1.4 Research Aim.....	10
1.5 Objectives .....	10
<b>Chapter 2: Research methodology and characterization techniques.....</b>	<b>11</b>
2.1 Materials used for sample preparation.....	11
2.2 Characterization Techniques .....	11
2.2.1 Scanning Electron Microscopy (SEM).....	11
2.2.2 Tensile/Compression Testing .....	14
2.3 Characterization of genuine ceramic tile(s).....	16
2.4 Optimization of fabrication conditions at a lab scale .....	19



2.5 Fabrication and assembly of self-fabricated ceramic tiles on imported backing plate.....	23
<b>Chapter 3: Results and discussions.....</b>	<b>27</b>
3.1 Specification of pure Alumina.....	27
3.2 SEM Analysis of Pure Alumina and Additives .....	27
3.3 Analysis of fabricated samples .....	29
3.3.1 SEM Analysis of fabricated Samples .....	29
3.3.2 Densification Values of Sintered Samples .....	30
3.4 Results of Mechanical Testing.....	37
3.4.1 Hardness values of fabricated sample.....	38
3.4.2 Compressive strength and Young’s Modulus of fabricated samples.....	42
<b>Chapter 4: Ballistic testing.....</b>	<b>45</b>
4.1 Testing Standards.....	46
4.2 Experimental Setup.....	47
4.2.1 Case 1: Ceramic tiles having thickness = 10 mm.....	48
4.2.2 Case 2: Ceramic tiles having thickness = 5 mm.....	49
4.3 Live Ballistic testing of the locally fabricated samples .....	49
4.4 Comparison with literature .....	54
<b>Conclusion.....</b>	<b>55</b>
<b>References.....</b>	<b>56</b>

# List of Figures

Figure 1: Usage of ceramic armour from protection materials .....	1
Figure 2: Classes of Composites .....	5
Figure 3: Components of composite armour .....	6
Figure 4: Schematic diagram of SEM [33].....	13
Figure 5 : Physical appearance of genuine ceramic tile .....	16
Figure 6 : XRD of Genuine ceramic tile .....	17
Figure 7 : Comparison of XRD analysis of genuine sample with standard alumina	17
Figure 8: SEM image of genuine ceramic tile.....	18
Figure 9: Laser spectroscopy of genuine ceramic tile .....	18
Figure 10: General P/M process scheme followed for the fabrication of samples [35] .....	19
Figure 11 : A planetary ball mill .....	20
Figure 12 : A planetary ball mill used to mill/mix powder samples .....	20
Figure 13 : A manual hydraulic press used to make green compacts.....	21
Figure 14 : Circular die used to press powders to green compacts .....	21

Figure 15 : Furnace used for de-binding ceramic compacts.....	22
Figure 16 : High temperature furnace used to sinter the samples .....	22
Figure 17 : Samples in upper row from left to right denoted as sample 1 and 2. Samples in lower row from left to right denoted as sample 3 and 4 respectively .....	23
Figure 18: Hexagonal die .....	24
Figure 19 : Samples after the de-binding process .....	24
Figure 20: Sintered hexagon samples.....	25
Figure 21 : Top and side view of the panels used .....	25
Figure 22 : Alumina tiles-panel assembly fabrication.....	26
Figure 23 : SEM of the starting powders.....	28
Figure 24: SEM images of the samples sintered .....	30
Figure 25: Densification values of sintered sample 1 .....	32
Figure 26: Densification values of sintered sample 2 .....	32
Figure 27: Densification values of sintered sample 3 .....	33
Figure 28 : Densification values of sintered sample 4 .....	33
Figure 29: Densification values of sintered samples @ <1600 °C.....	35
Figure 30: Densification values of sintered samples @ 1600 °C.....	35

Figure 31: Densification values of sintered samples @>1600°C.....	36
Figure 32: Average hardness values of the samples fabricated @<1600 °C.....	39
Figure 33: Average hardness values of the samples fabricated @1600 °C.....	39
Figure 34: Average hardness values of the samples fabricated @>1600 °C.....	40
Figure 35: Average hardness values of sample 1 .....	41
Figure 36: Average hardness values of sample 2 .....	41
Figure 37: Average hardness values of sample 3 .....	42
Figure 38 : Average hardness values of sample 4 .....	42
Figure 39: Compressive Strength of Sintered Samples .....	43
Figure 40 : Young's Modulus of Sintered Samples .....	44
Figure 41: 7.62 mm armour Piercing Bullet.....	47
Figure 42: Live firing setup for ceramic tiles having thickness = 10 mm.....	48
Figure 43: Live firing setup for ceramic tiles having thickness = 5 mm.....	49
Figure 44 : Examples of BFS systems.....	50
Figure 45 : Fixation of ballistic panel for testing .....	51
Figure 46 : Ballistic panel after first shot .....	51

Figure 47 : Ballistic panel after second shot .....52

Figure 48: Back side of the panel after ballistic test .....53

Figure 49: Side view of the panel showing trauma after testing .....53

# List of Tables

Table 1 : List of additives used.....	11
Table 2 : Characteristics of the starting Al <sub>2</sub> O <sub>3</sub> powder .....	27
Table 3: Characteristics of base material and additives .....	28
Table 4: Composition of fabricated samples .....	29
Table 5: Densification values of sintered samples .....	37
Table 6: Hardness values of the fabricated samples.....	38
Table 7 : Compressive strength values of the samples fabricated.....	43
Table 8: Comparison of literature with current research work.....	54

# Chapter 1:

## Introduction

In this dissertation, the research work has been divided into two phases. First phase deals with indigenous fabrication and characterization of composite ballistic armour while second part deals with the live experimentation on ceramic tiles against armour piercing projectiles.

### 1.1 Background

For applications pertaining to combats and warfare, resistance to impact penetration and resilience ability to shock are very vital. Study of response of armour materials to shock and impact play dynamic role in developing improved armour for civilian and military applications. The designing, development and manufacturing of bullet proof materials involve study of response of materials under consideration so that their shock resilience can be enhanced. Weapon and bullets are being improved from time to time, which require improvement in protection against newly developed threats as mentioned in figure 1.

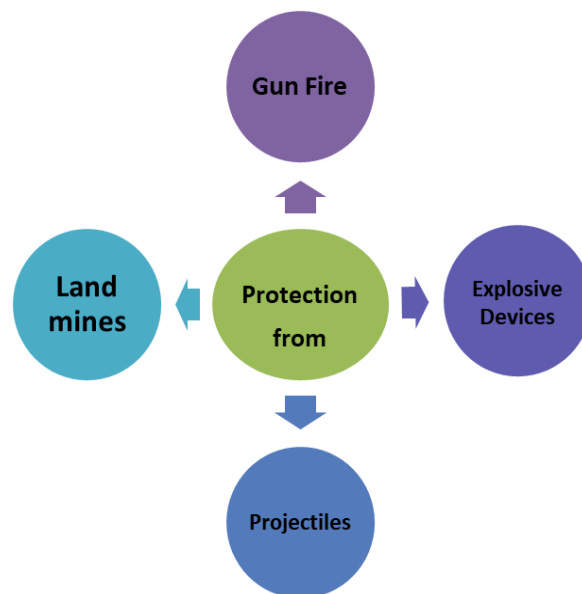


Figure 1: Usage of ceramic armour from protection materials

Pakistan has been fighting against terrorism since last two decades and has eliminated it to a greater extent. But still many security threats prevail. To increase protection armoured vehicles, bullet proof vests and guard posts, security forces are in search of different ways to protect their civilians and military personnel safe from threats especially small calibers. Usage of armour systems is one of the primary and efficient defense approaches being deployed. But even most effective armoured vehicles have been compromised which indicated requirement for development of better alternative materials for upgraded protection. High strength armoured plates are usually used for protection of personnel in armoured vehicles which cause increase in weight and difficulty in mobility. Also, such plates characteristically fail due to softening of material by strong agglomeration of plastic deformation undergoing major adiabatic heat in few shear planes. Ceramic materials have enough toughness to beat the incoming projectiles with less weight plenty. The objective of our research is to study and fabricate indigenously composite ballistic armour. High strength ceramics are used to defeat incoming projectiles so that no penetration or min penetration in backing plate occur[1]. The requirements for designing an armour protection need the application of that particular protection system. The essential aspects of a protection system include its cost, protection capability, weight and mobility. Different research scholars analyzed the ballistic response and performance of metals, polymers, ceramics and their composites [2]–[6]. Even with availability of raw materials, only limited research has been carried out to fabricate ceramics indigenously. Light weight ballistic armour is being employed for the safety of military and security personnel. This lightweight armour is composed of composite sheets assembled together to provide maximum protection against high velocity moving objects/projectiles. In Pakistan, HIT, Heavy Industries Taxila is the leading consumer and suppliers for this armour equipment. Modern lightweight armour is attached to armoured vehicles and is also worn in bullet-proof vests for protection to military and security personnel throughout the country. When attached to vehicles, they provide protection from gun fire, explosive devices and projectiles. The challenge is to offer the highest level of protection without increasing weight. Modern ceramic composites, being light weight, have largely replaced steel as the non-structural armour in combat vehicles and vests. The new generation of textile



fibres i-e Kevlar 16 was used in 1965. This fibre has shown more strength than steel and it provide much more protection against bullets [7].

The demand of composites is increasing because of following features like lightweight-ness, high strength to weight ratio and high resistance against corrosion.

In modern, high end bullet-proof armour system, the component that is responsible for projectile shielding and providing protection is a ceramic tile. Advanced ceramics are high strength sintered monoliths that have the ability to absorb high impact values without deforming. These ceramics, in the form of tiles, are joined together by high strength adhesive and sandwiched in a reinforced polymer structure in order to obtain a high specific performance armour system [8]. Despite having raw material reserves, the industrial and academic sectors of Pakistan do not possess the required infrastructure to fabricate such ceramic systems of a sufficient quality. Thus, defense industries rely on foreign imports in order to utilize such products. Although sufficient for the short term, dependence on imports comes with a lot of risks regarding an unpredictability in material availability for the long term. Additionally, imported fabricated ceramics are expensive and are subject to changes and devaluation of Pakistan's currency in the international market. Therefore, the purpose of this project was to explore an indigenous route towards the fabrication of ceramic tiles, particularly for armour application. The outcome of this project are high strength ceramic tiles that have been locally fabricated, tested and optimized, to be used for composite armour systems. The HIT spends approximately \$600,000 - \$1,000,000/- each year on armouring of vehicles and bullet-proof vests. Significant savings in this expenditure can be made possible if the major factor of the composite armour system, which are the ceramic tiles manufactured locally. This is thought to not only result in reducing an overall import bill but will also provide stability in the availability of such products. An additional advantage of this project is that certain other companies/products can benefit through a local establishment of this technology. Pakistan has a dwindling manufacturing clout when it comes to advanced structural ceramics. These ceramics find their uses in aerospace structural components, tools for the cutting/wear industry, automotive engine components and insulators for different applications. However, a recent recession has seen the

ceramic sector become confined to the manufacture of only tiles and bricks for households. It is believed that an indigenization of this technology can revive many other local sectors of ceramic manufacturing.

## 1.2 Literature Review

Ballistic threats are improving day by day which obviously demands improvements in protection. Many types of body covering have been formed to provide protection against these ballistic threats. But different kinds of ballistic protections are not similarly safe. This means that while selecting a ballistic body shield be aware that it is giving a complete protection [4]. To choose the ballistic body shield, the impact behavior of that shield influenced by the following factor should be considered.

- Bullet parameters
- Armour specifications

A bullet can affect ballistic performance via its tip shape, mass, angle and speed. Armour gives its performance from its area, thickness, density, composition and constituent materials. Testing conditions also play an important role [9].

There are different criteria which can be used when selecting material for an armour system while remaining in allowable price and volume. None of material could be selected as best material for armouring [10]. Because a material providing protection against a threat can be inadequate for threat in any other threat scenario, particularly if either or volume or both are required to be lessened [9].

Following materials are commonly used in armouring:

- **Rolled Homogenous Armour:** Rolled homogenous armour is made up to hardened steel and a high velocity projectile can't shatter this material [11].
- **Ceramics:** Ceramics are commonly used in armouring especially as composite with different materials. Silicon Carbide, Silicon Nitride, Boron Carbide, Aluminum Oxide and Tungsten Carbide are normally used in armouring application [12].

- **Glass:** Glass commonly labeled as bullet proof glass is also used for transparent armour in vehicles and other structures built for surveillance [13].
- **Aluminum:** Aluminum metal is usually used in light weight armoured vehicles [14].
- **Depleted Uranium:** Depleted Uranium of high density is sandwiched between armour plates in tanks for higher protection [15].
- **Plastic:** Plastic can deflect incoming projectile's trajectory and are enormously effective against armour piercing projectiles [16].
- **Titanium:** Titanium is also considered as one of the potent armouring material but due its higher cost, it is not economical to use [17]
- **Composite Materials:** Composite materials are widely used in armouring and reinforcing applications [18]. Three main classes of composite materials are depicted in figure 2 which are structural composites, fiber reinforced composites and particle reinforced composites.

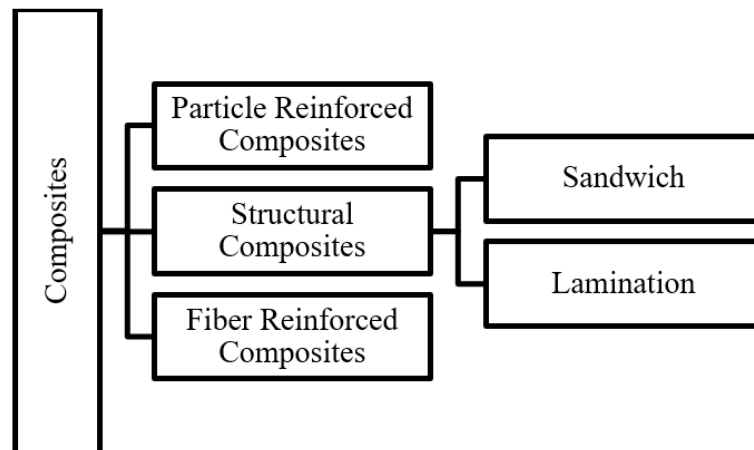


Figure 2: Classes of Composites

Component of composite armour consist of four layers. First one is splinter foil. Then ceramic tile is combined with the glue to make it intact with backing plate as shown in figure 3. Splinter foil is used to keep the ceramic tiles intact with the remaining system. Just beneath the splinter foil is the ceramic tile which crush the incoming projectile into pieces. These ceramic tiles are mounted on backing plate

that is also called soft armour by using a glue or epoxy. Backing plate is used to absorb the remaining kinetic energy and saves the personnel from trauma.

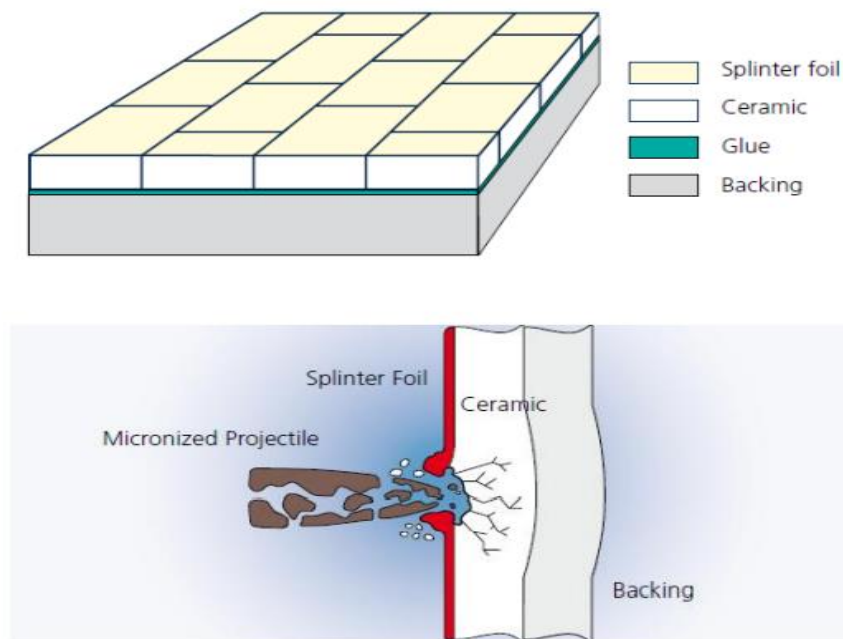


Figure 3: Components of composite armour

Various factors affect the ballistic performance of different types of armours, which includes:

- Bullet materials, shape and size
- Bullet mass and diameter
- Bullet velocity

Based on level of protection, many different materials can be used in different ways. High-performance fibres and their hybridization have developed new emerging potential for composite materials. Therefore, composites materials are recognized as superior materials of the 21st century. They have high damage tolerance, lighter in weight and stiffer in nature as and more efficient compare to steel [19].

Various latest body armour filaments are Aramid (trade name, Kevlar, Twaron, Technora), the high-performance polyethylene (Dyneema), High strength nylon, poly (p-phenylene2,6 benzo isoxazole). Ultra-high molecular weight polyethylene

(UHMWPE ) (Dyneema) was selected as backing plate because it provides the best combination of the protection and weight [20].

Ceramics have modest tensile strength and they depict brittle fracture behavior due to this reason they cannot used stand-alone in armour applications. They require a support by using backing material which is more ductile and can absorb the kinetic energy. [1].

Karandikar et al. [2] studied the Effects of novel geometric designs on the ballistic performance of ceramics. He found that ceramics are lightweight and have high hardness. He deduced that efficiency of armour system can be enhanced by combining the ceramics along with an ultrahigh molecular weight polyethylene (UHMWPE) backing plate.

In this research work UHMWPE panels are used to provide the best combination of the protection and weight. The UHMWPE panels were procured from abroad and used for protection purposes. Performance measurements and analysis of imported armour were also conducted to analyzed their properties by using Scanning electron microscope (SEM), X-Ray Diffraction (XRD) technique and hardness testing [21].

In the recent years, a great work has been carried out for the development of ceramic based material especially on Alumina.  $Al_2O_3$  is used as base material for manufacturing of tiles as it is easily available, high-quality wear-resistant and shock resistance protective material [22],[23].

Most of research work focused on adding reinforcing material in alumina matrix due to low fracture toughness, brittle fracture behavior and low sintering behavior [24].

Different additives have been used and studied by different authors [25]–[27]. Three different additives were used for sample (ceramic tile) preparation by using different compositions of  $Al_2O_3$  with MgO,  $TiO_2$ , and  $SiO_2$  powders. The addition of these powders promoted sintering and restricted excessive grain growth caused by using longer sintering cycles. then these tiles were combined with UHMWPE using structural epoxy.

To increase the fracture toughness and strength, SiC whisker (SiCw)-reinforced  $\text{Al}_2\text{O}_3$  is gaining much more attention. Whisker reinforcement can minimize the catastrophic brittle failure of  $\text{Al}_2\text{O}_3$  via a range of toughening mechanisms, such as crack deflection, whisker pullout and bridging [28],[29].

Lee et al. [30] studied the Properties of alumina matrix composites reinforced with SiC whisker and carbon nanotubes and they found that the effects of MWCNTs addition on the mechanical properties of  $\text{Al}_2\text{O}_3$  were trivial, whereas those of SiCw were significant.

Parchoviansky et al. [31] investigated the Microstructure and mechanical properties of hot pressed  $\text{Al}_2\text{O}_3/\text{SiC}$  nanocomposites. They found that the mechanical properties of  $\text{Al}_2\text{O}_3/\text{SiC}$  nanocomposites have been improved very well, when micro or nano SiC particles were incorporated as compared to monolithic  $\text{Al}_2\text{O}_3$ .

Based on literature review,  $\text{SiO}_2$ , MgO and  $\text{TiO}_2$  additives were chosen as a additive in Alumina with different compositions to make the indigenously armour material. Then ceramic samples were prepared and characterized by using high-tech characterization techniques for ballistic protection.

After this, by using purchased UHMWPE, composite panels were assembled and tested using standard conditions. Ballistic testing of indigenously fabricated composite armour was conducted by using high speed camera.

For the testing of these prepared samples, different testing method are available. There are extensive choices of standards available for ballistics security levels. Generally, every nation has its own arrangement of least measures for ballistic, spike and edged cutting edge body reinforcement.

The two more commonly used guidelines for body armour are presented by

1. US National Institute of Justice (NIJ) and
2. the UK Centre for Applied Science and Technology (CAST, once in the past HOSDB) [32].

These are generally held to be the world leaders in institutionalizing body armour. Testing techniques are regularly shared between the two, so body armour that satisfies the guidelines of one will meet the prerequisites of the equation. CAST and NIJ work in participation, with CAST dealing with a spike and edged cutting edge measures while NIJ handles ballistic reinforcement. NIJ level III is used for the testing according to the requirement of end user [2].

An added advantage of this project is to introduce the technology of advanced ceramics in the country. The successful completion of this project is expected to contribute to the knowledge of processing and fabricating advanced ceramics for a wide variety of applications.

This project is aimed to figure out a pathway of fabricating relatively low-cost composite armour. Currently the project team had been relying on small scale powder samples to begin with, which are much more expensive, size wise, as compared to large scale orders. Since the processing and manufacturing of ceramic tiles for ballistic armour is done locally, such costs in addition to shipment and custom taxes could be minimized. It is believed that upon the start of production of ceramic tiles, such a process is also going to benefit the local industry in terms of local production of advanced ceramics.

Based on above discussed background and literature of research work, aim and objectives of this research work are defined as follows.

### **1.3 Problem Statement**

By analyzing the literature review, following problem statement was set as under:

The industrial and academic sectors of Pakistan do not possess the required infrastructure to fabricate such ceramic systems of a sufficient quality. Thus, defense industries rely on foreign imports in order to utilize such products.

## **1.4 Research Aim**

The aim of research work is defined to minimize the cost and foreign dependency by manufacturing ballistic ceramic tiles indigenously using local resources, and to check ballistic response of the tiles against armour projectiles

## **1.5 Objectives**

The objectives of this research are set in the light of problem statement and aim of this research work.

1. Characterization of existing ceramic tile(s)
2. Optimization of fabrication conditions at a lab scale
3. Fabrication and assembly of self-fabricated ceramic tiles on imported backing plates
4. Ballistic testing of the locally fabricated samples



## Chapter 2:

# Research methodology and characterization techniques

### 2.1 Materials used for sample preparation

Alumina is used as base ceramic material. Bauxite ores are present and found in different regions of Pakistan, and those ores can be used for the refinement and subsequent production of  $Al_2O_3$ .

Based on literature following different additives are incorporated in alumina for preparation of ceramic composited armour. The addition of these powders promoted sintering and restricted excessive grain growth caused by using longer sintering cycles

Table 1 : List of additives used

Additives	Effects
$TiO_2$	Densification enhancement
$MgO$	Densification enhancement + grain growth inhibition
$SiO_2$	Densification enhancement

The UHMWPE panels were procured from abroad used as backing plate. Yd 127 is used as epoxy and 7301 hardener. Both are used in certain portion to attach the composite sample with backing plate.

### 2.2 Characterization Techniques

Following different characterization techniques are used for analysis of lab scale samples.

#### 2.2.1 Scanning Electron Microscopy (SEM)

Scanning electron microscope is one of the most important characterization techniques to analyze structure and morphology at nanometers level. High energy

electrons are bombarded on the surface of material. SEM is used to determine the surface and cross section of material/samples. Samples were coated with gold and analyzed at 10 mm distance and with current of 90 mA.

Scanning electron microscope (SEM) is used to analyze the structure and morphology of materials. High energy electrons are focused on the surface of the material. The analysis is performed to determine the surface and cross-sectional morphology.

#### **2.2.1.1 Working principle**

High energy electrons are focused on the surface of material. For image of material secondary electrons are used while backscattered electrons are used for phase determination. The secondary electrons show the morphology and topology of membrane material.

Image formation in SEM depends upon detector. Signal (S) is measured by counting electrons falling on detector. The noise (N) reduces the signal and quality is diminished. By increasing number of counts, quality can be improved since it is ratio of signal to noise (S/N).

SEM forms an intensity map which is two dimensional. Each pixel is indicative of a point on sample which is related to the intensity of sample.

SEM forms a two-dimensional intensity map and each pixel on the map is representative of a point of the sample which is directly related to the intensity of the signal. It is not possible for SEM to generate a true image rather the image is displayed electronically. SEM determines two characteristic features of a material: Morphology & topography.

#### **2.2.1.2 Instrumentation**

SEM has following components as mentioned in figure 4 [33]

- Display
- Vacuum system

- Detector
- Scanning system
- Electron column
- Electronic control

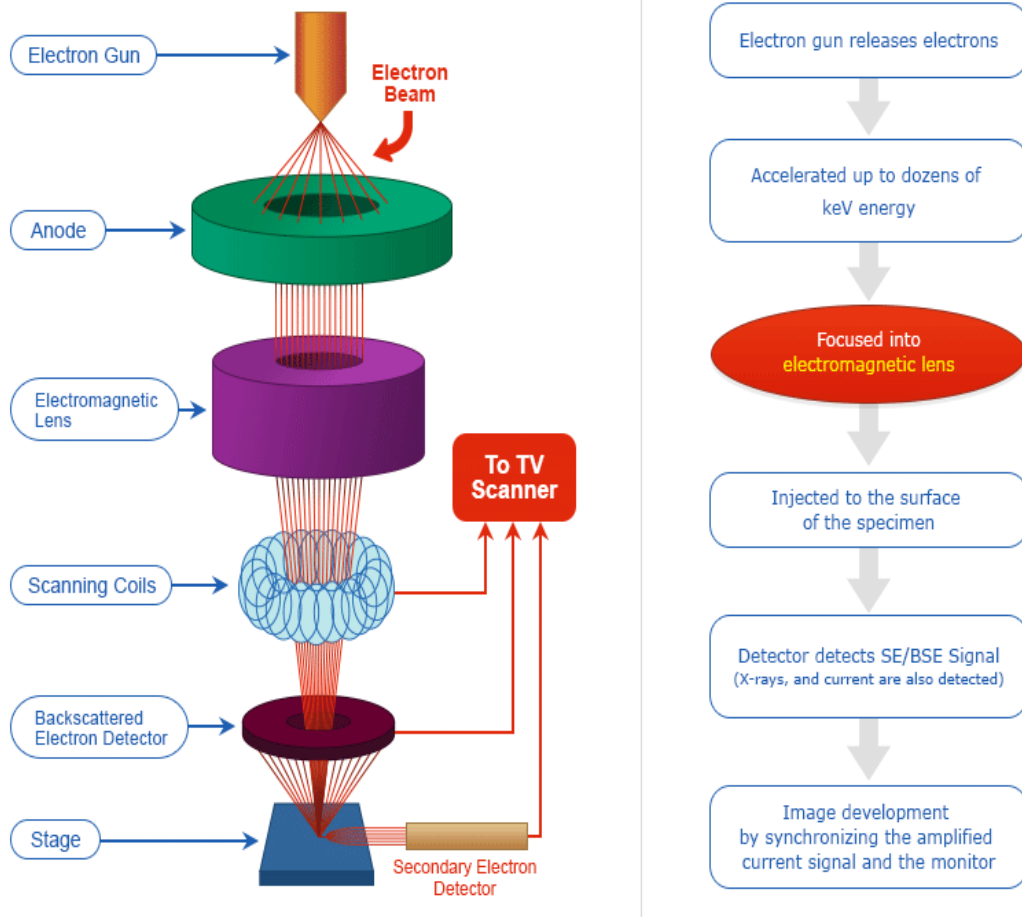


Figure 4: Schematic diagram of SEM [33]

### 2.2.1.3 Information provided by SEM

SEM analysis provides the following information about the sample

- Morphology: related to the size and appearance
- Topography: related to the surface characteristics of the sample

### 2.2.2 Tensile/Compression Testing

This technique is used to measure the mechanical stability of material. It is used to predict the behavior of the sample under loading. In this test material undergoes through stress and the resulting deformation produced from stress is measured. It is commonly used to determine the maximum stress that a material can withstand without failure. Ultimate tensile strength and maximum elongation are directly measured with the help of tensile test. With the help of these measurements young's modulus, yield strength and strain hardening characteristics of the sample can be determined.

#### 2.2.2.1 Working Principle

An axial force is applied on the sample of original length  $L_0$  to elongate it. The specimen to be tested is placed between jaws of UTM and force in axial direction is applied while recording the resulting strain through computer software. Strain recording is done until material fracture. Relationship between stress and strain is determined through change in length.

Stress is defined by the following equation

$$\text{Stress} = \frac{\text{Force}}{\text{Area}}$$

While strain is defined by the following equation

$$\text{Strain} = \frac{\text{Change in length}}{\text{Original length}}$$

### 2.2.2.2 Instrumentation

It consists of the following parts as mentioned in figure 5 [34]

- Load cell
- Moving cross head
- Fixed cross head
- Base and actuator
- Frame
- Crosshead
- Gripping Jaws
- Extensometer
- Specimen
- Engine
- Gear
- Screws

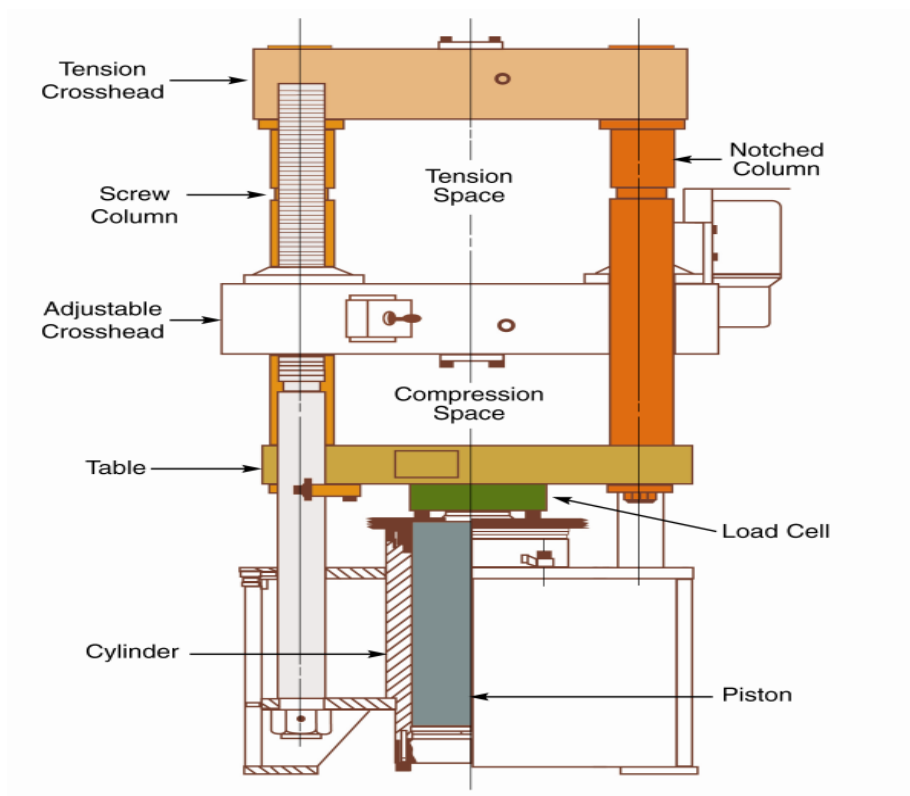


Figure 5: Schematic Diagram of Tensile Strength Tester [63]

### 2.2.2.3 Applications

Mechanical testing is usually done to get a knowledge about material properties like

- Elasticity
- Toughness
- Ductility
- Resilience

### 2.3 Characterization of genuine ceramic tile(s)

Genuine tiles that were used for characterization to set a base line for indigenous development of the ballistic ceramic tile is shown below. Physical appearance is like it is made up of alumina but characterization is required before any conclusion.



Figure 5 : Physical appearance of genuine ceramic tile

XRD, SEM and Laser Spectroscopy were performed to take a fair idea about the composition of the genuine tile.

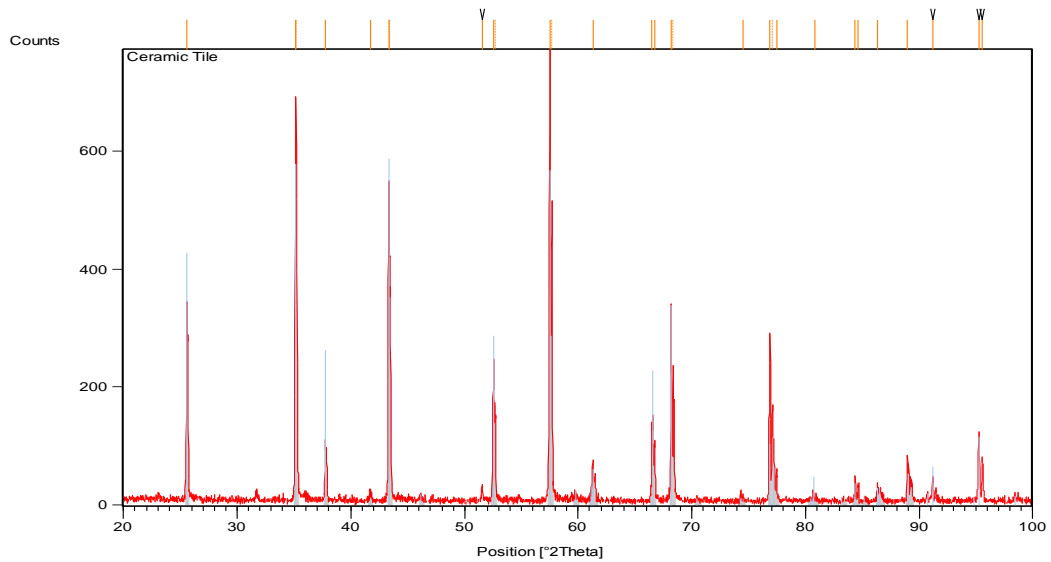


Figure 6 : XRD of Genuine ceramic tile

These are the XRD peaks of the genuine tiles. When it was compared with the standard peaks of corundum that is alpha alumina, it can be seen in the fig below those peaks of the genuine tile is at the same position with the peaks of alpha alumina. This confirms that genuine tile is made up of pure alumina.

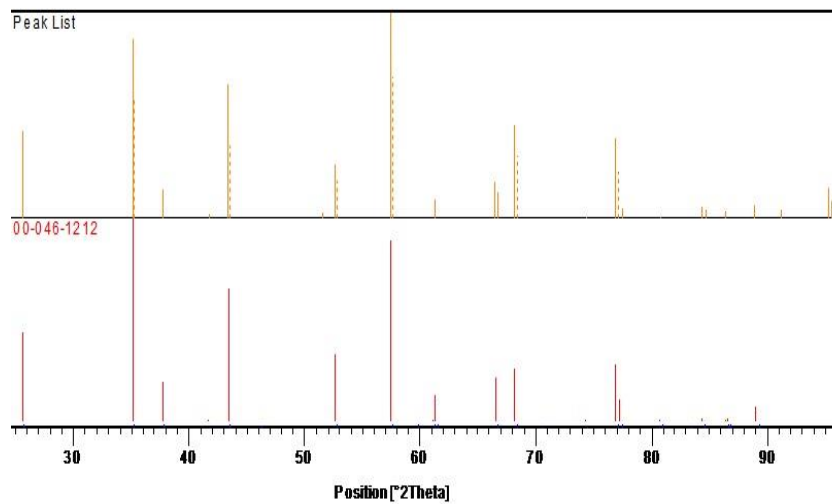


Figure 7 : Comparison of XRD analysis of genuine sample with standard alumina

To check the morphology and size of the particles SEM was performed and image of the SEM is shown below. The particle size is around 10 microns.

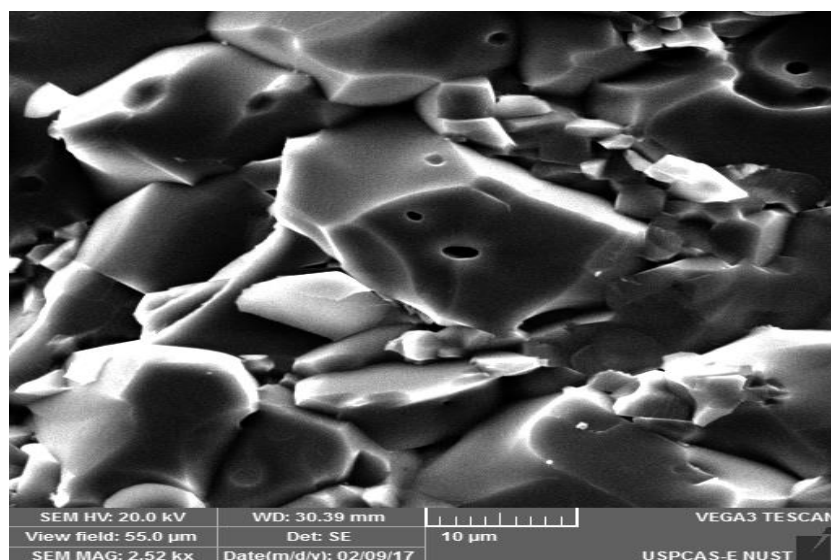


Figure 8: SEM image of genuine ceramic tile

To reconfirm the composition of the genuine tile, laser spectroscopy was performed. Major peaks in the fig can be seen that are of aluminum and oxygen which confirm that genuine ceramic tile is made up of alumina. Mg peak is also present that may be the impurity or the additive that was used for manufacturing of the genuine tile.

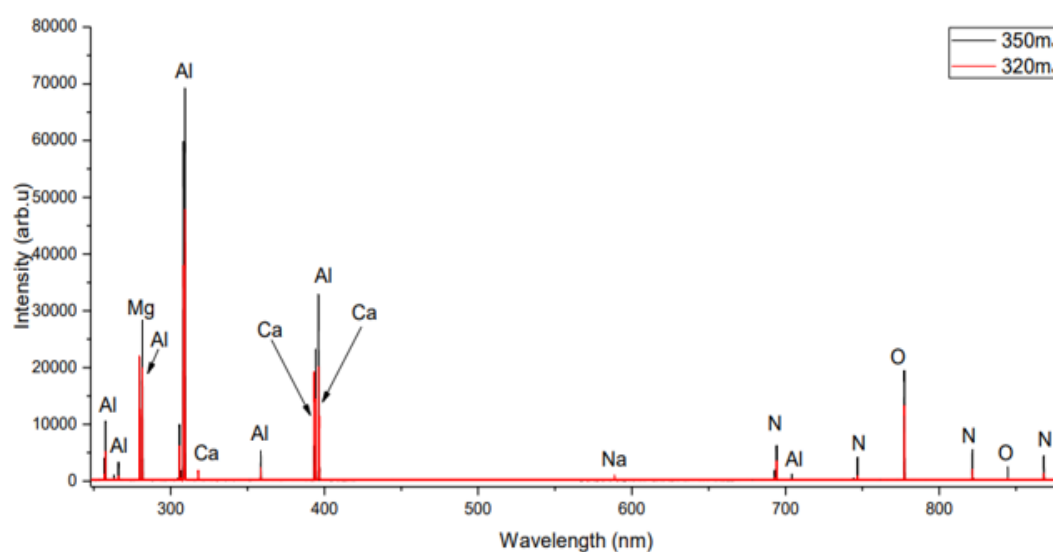


Figure 9: Laser spectroscopy of genuine ceramic tile



## 2.4 Optimization of fabrication conditions at a lab scale

The methodology followed for the preparation of samples can be seen in the general P/M process is shown in figure 11.

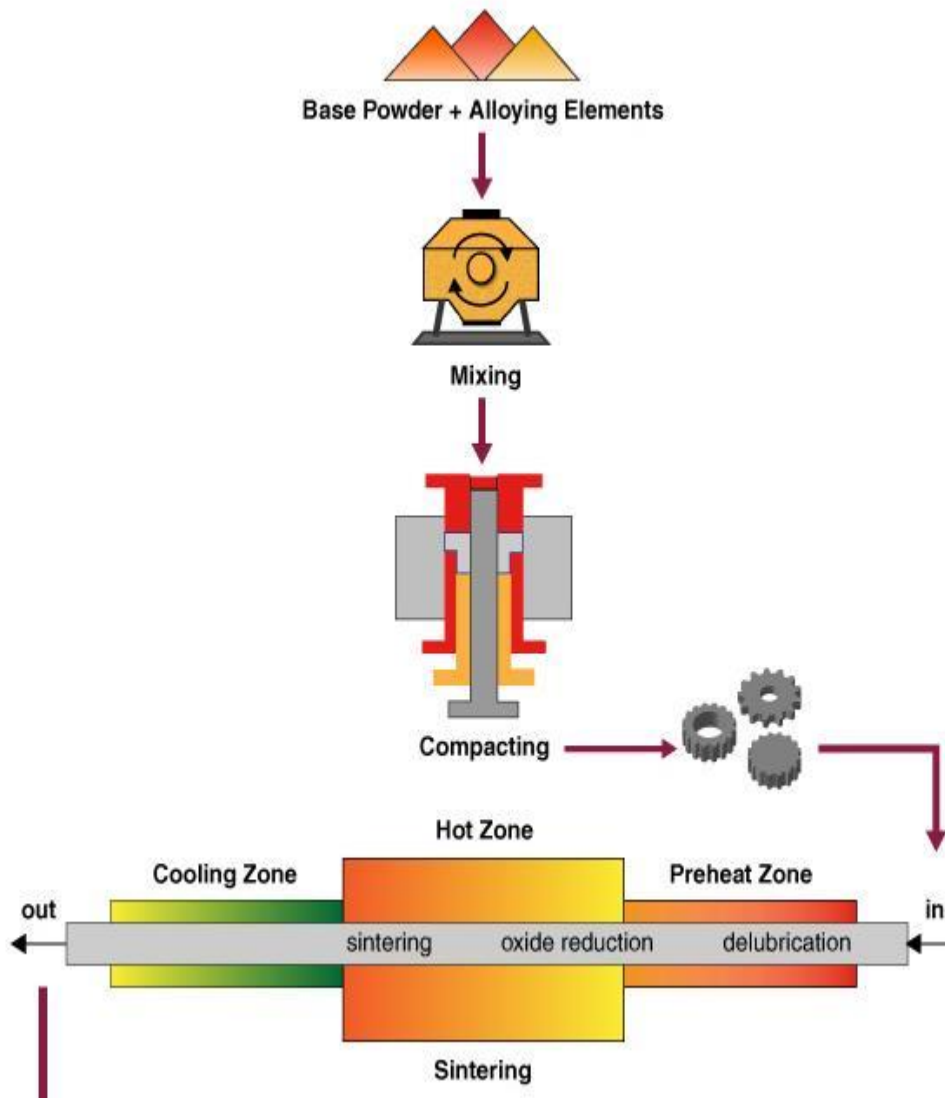


Figure 10: General P/M process scheme followed for the fabrication of samples [35]

The process begins with mixing/milling of powdered samples desired in specific compositions. They are then subjected to uniaxial pressing using hardened steel dies, where a force is applied to press the powder in the compact shape known as green compact. The green compacts are then sintered in a high temperature furnace that

de-binds and later densifies the powder into bulk sintered compacts with high densification. The equipment used for powder mixing/milling and compaction can be seen in the figure 12,13 and 14 respectively.



Figure 11 : A planetary ball mill



Figure 12 : A planetary ball mill used to mill/mix powder samples



Figure 13 : A manual hydraulic press used to make green compacts

The dies used to press the powders can be seen in the figure 15.



Figure 14 : Circular die used to press powders to green compacts

The furnace that was used to de-bind the ceramic samples can be seen in the figure 16 and figure 17.



Figure 15 : Furnace used for de-binding ceramic compacts



Figure 16 : High temperature furnace used to sinter the samples

The pressed and de-binded samples were subjected to high temperature sintering using a hot press furnace as seen above. The process of sintering compacts the powdered samples until they form uniform dense compacts. Four different sample

types were prepared using different compositions of  $\text{Al}_2\text{O}_3$  with  $\text{MgO}$ ,  $\text{TiO}_2$ , and  $\text{SiO}_2$  powders as shown in figure 18. The addition of these powders promoted sintering and restricted excessive grain growth caused by using longer sintering cycles. For brevity, results pertaining to three different compositions will be discussed here.



**Sample 1**



**Sample 2**



**Sample 3**



**Sample 4**

Figure 17 : Samples in upper row from left to right denoted as sample 1 and 2. Samples in lower row from left to right denoted as sample 3 and 4 respectively

## **2.5 Fabrication and assembly of self-fabricated ceramic tiles on imported backing plate**

A hexagonal shaped die was used to press the powder samples into hexagonal compacts. The die is shown in the figure 19.



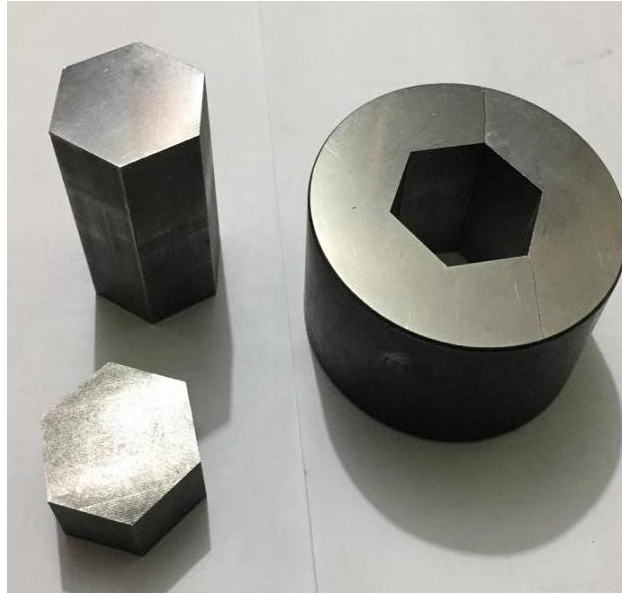


Figure 18: Hexagonal die

The hexagonal shaped samples were first subjected to calcination and a de-binding process, that is conducted over moderate temperatures. The samples after de-binding can be seen in the figure 20.



Figure 19 : Samples after the de-binding process

Finally, the hexagon shaped samples were subjected to the high temperature sintering conditions, optimized on a lab scale, and shown previously. The images of the completely sintered samples can be seen in figure 21.

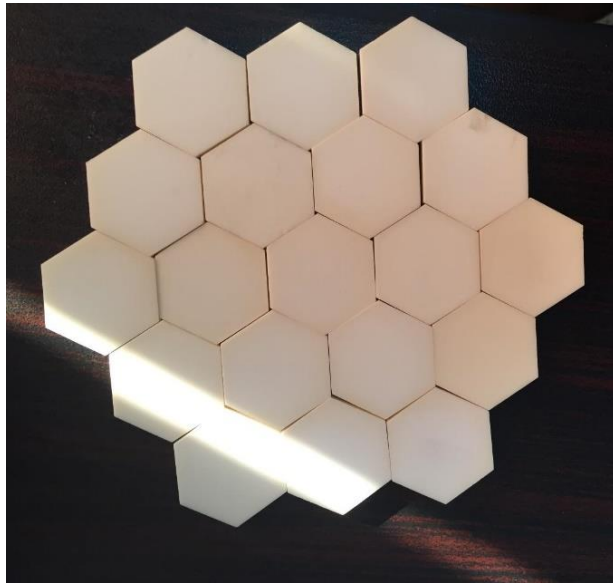


Figure 20: Sintered hexagon samples

The hexagonal samples were mounted on top of UHMWPE panels to provide the best combination of the protection and weight. The UHMWPE panels were procured from abroad. The figures 22 and 23 display the panel that was used and the  $\text{Al}_2\text{O}_3$  tiles-UHMWPE assembly.



Figure 21 : Top and side view of the panels used

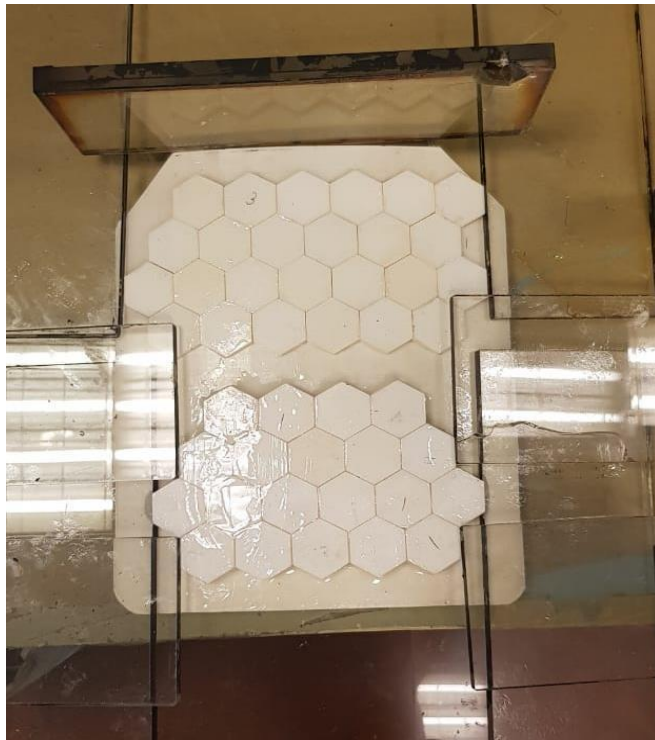


Figure 22 : Alumina tiles-panel assembly fabrication



## Chapter 3: Results and discussions

### 3.1 Specification of pure Alumina

The starting  $\text{Al}_2\text{O}_3$  powder used was sub-micron with high purity.  $\text{Al}_2\text{O}_3$  powder was purchased from Sigma Aldrich. The characteristics of alumina powder are presented in table 2.

Table 2 : Characteristics of the starting  $\text{Al}_2\text{O}_3$  powder

Quantity	Values
$\text{Al}_2\text{O}_3$ wt %	>99
$\text{Na}_2\text{O}$ wt%	<0.05
$\text{Fe}_2\text{O}_3$	<0.03
Apparent density ( $\text{g}/\text{cm}^3$ )	>0.95
D50 size ( $\mu\text{m}$ )	<0.6
Blank density ( $\text{g}/\text{cm}^3$ )	2.1-2.2

### 3.2 SEM Analysis of Pure Alumina and Additives

SEM analysis of alumina sample was performed to re-confirm the specifications provided by the manufacturer. It can be clearly seen in figure 18 that particle size of alumina is almost same as per specification provided by supplier.

The SEM images of the starting powders can be seen in the figure 24.

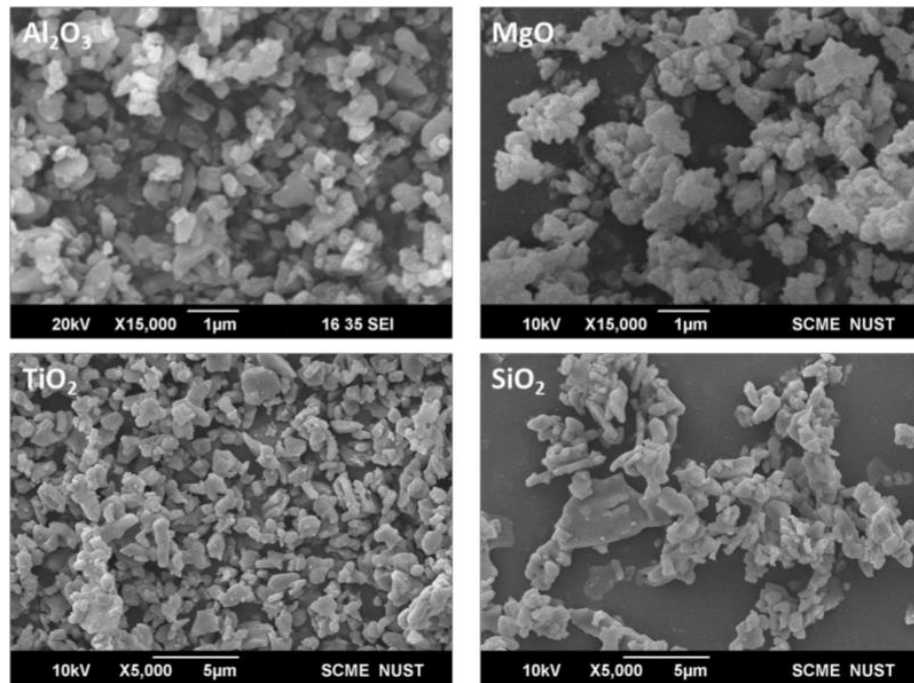


Figure 23 : SEM of the starting powders

The table 3 is showing the characteristics of base material and additives used in preparation of samples i-e SiO<sub>2</sub>, MgO and TiO<sub>2</sub>.

Table 3: Characteristics of base material and additives

Materials used	Morphology	Size range
Alumina	Irregularly shaped particles	<0.6 μm
MgO	Irregularly shaped particles	<0.1 μm
TiO <sub>2</sub>	Irregularly shaped particles	<0.2 μm
SiO <sub>2</sub>	Irregularly shaped particles	<0.5 μm

Different powders were used for sample preparation. Powders obtained from different sources were analyzed using SEM available in SCME. Alumina has irregularly shaped particles with size range less than 0.6 micrometer [36]. Particles of MgO has irregularly shaped particles with an average size less than 0.1 micrometer [37]. Particles of TiO<sub>2</sub> has irregularly shaped particles with an average size less than 0.2 micrometer [38] and similarly SiO<sub>2</sub> irregularly shaped particles having average size less than 0.5 micrometer [39].

### 3.3 Analysis of fabricated samples

Four different types of the samples were prepared to observe the effect of morphology, densification, mechanical properties and ballistic testing by sintering at three different temperatures  $<1600\text{ }^{\circ}\text{C}$ ,  $1600\text{ }^{\circ}\text{C}$  and  $>1600\text{ }^{\circ}\text{C}$ . Following table 4 is showing the composition of the fabricated samples.

Table 4: Composition of fabricated samples

Sr. No	Nomenclature	Composition
1	Sample 1	Pure Alumina
2	Sample 2	Alumina + $\text{TiO}_2$
3	Sample 3	Alumina + $\text{TiO}_2$ + $\text{MgO}$
4	Sample 4	Alumina + $\text{TiO}_2$ + $\text{SiO}_2$

#### 3.3.1 SEM Analysis of fabricated Samples

The sintered samples were polished, etched and studied under a SEM to reveal the grain structure of the samples. The figure 25 shows the microstructure of the sintered samples.

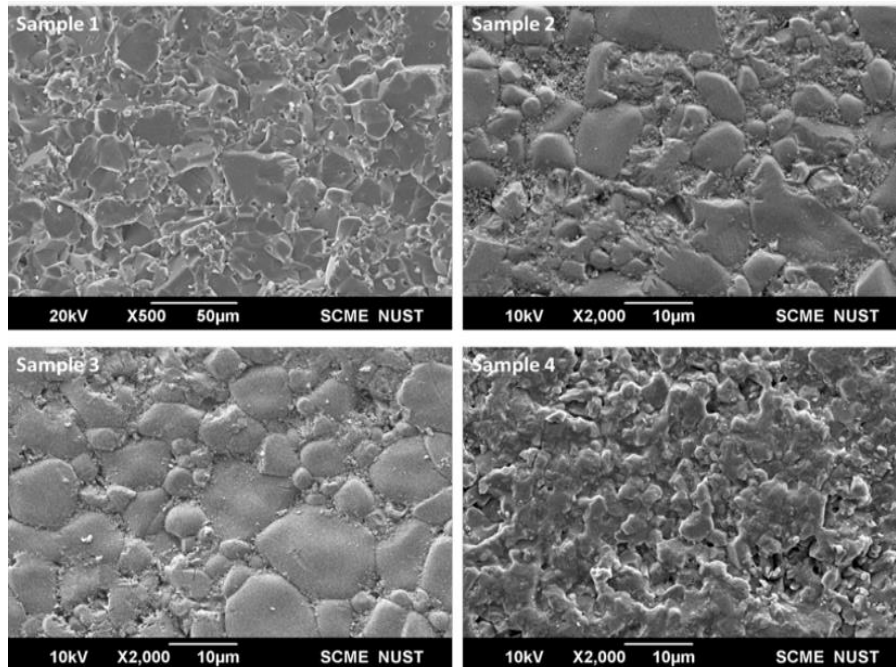


Figure 24: SEM images of the samples sintered

In SEM image, sample 1 that is pure alumina sintered at  $>1600\text{ }^{\circ}\text{C}$  and still porosity can be seen in the structure. Sintering linear shrinkage increased with increasing sintering temperature, resulting in higher volumetric changes [40]. Thus, this effect increases densification and reduces total porosity while improving the tensile strength of the porous alumina ceramic composites.

### 3.3.2 Densification Values of Sintered Samples

To further improve the mechanical properties additives are added to the alumina which not only increase the densification but also the other mechanical characteristics as well. So, in order to enhance the properties  $\text{TiO}_2$  was added to pure alumina and sintered at  $>1600\text{ }^{\circ}\text{C}$  and named as sample 2.

The mechanism involved is the densification enhancement and forming a solid solution resulting in the mechanical properties being improved in comparison of those pure alumina. But still few abnormal growths of the grains can be seen in the image. Similarly, addition of  $\text{MgO}$  and  $\text{TiO}_2$  was done in pure alumina at the time of mixing and then sintering was done at the same temperature. Scientists have figured

out that adding low amounts of MgO can lead to increased compressibility of alumina [41].

The prevalent theory is that MgO prevents grain growth by decreasing the grain boundary mobility and enhance densification. All the grains are showing regular growth as can be seen in sample no 3 image.

Fore going in view of above, SiO<sub>2</sub> and TiO<sub>2</sub> was added to the pure alumina and again sintering temperature was the same because that temperature gave the best results.

Addition of silica also good in increases the densification but on the other hand decreases the mechanical properties of the ceramic composite due to glassy phase.

### **3.3.2.1 Effect of temperature on densification**

Bar graph below in figure 26 shows densification of the pure alumina (sample 1) with temperature. Bar graph is showing the percentage densification obtained at lower temperature < 1600°C is 83.15 and increased to 96.9 percent by increasing the sintering temperature.

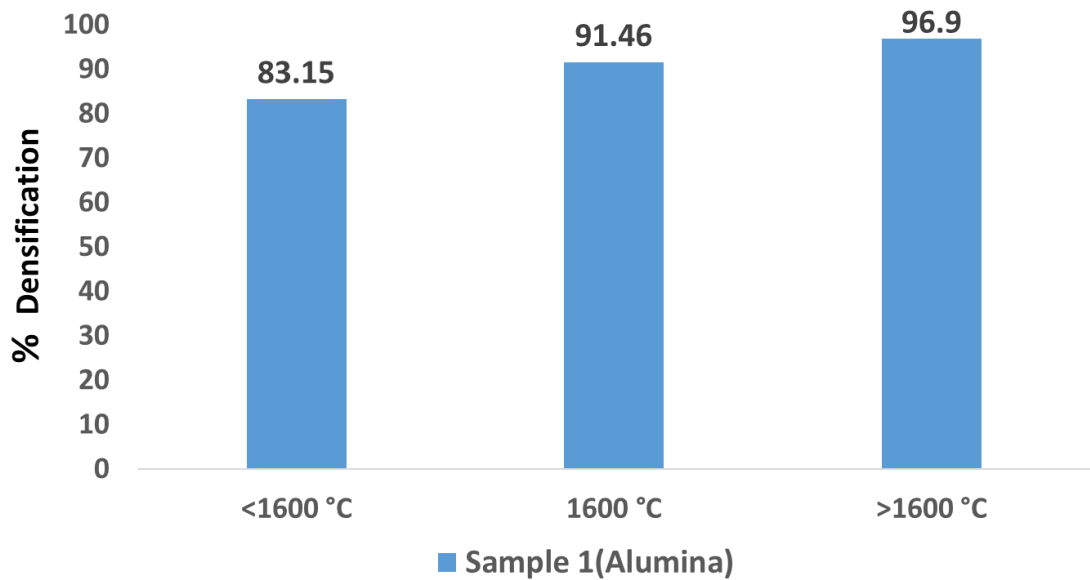


Figure 25: Densification values of sintered sample 1

Figure 27 below shows densification of the alumina + TiO<sub>2</sub> (sample 2) with temperature. It can be seen that percentage densification obtained at temperature <1600°C is 91.46 and increased to 97.9 percent by increasing the sintering temperature.

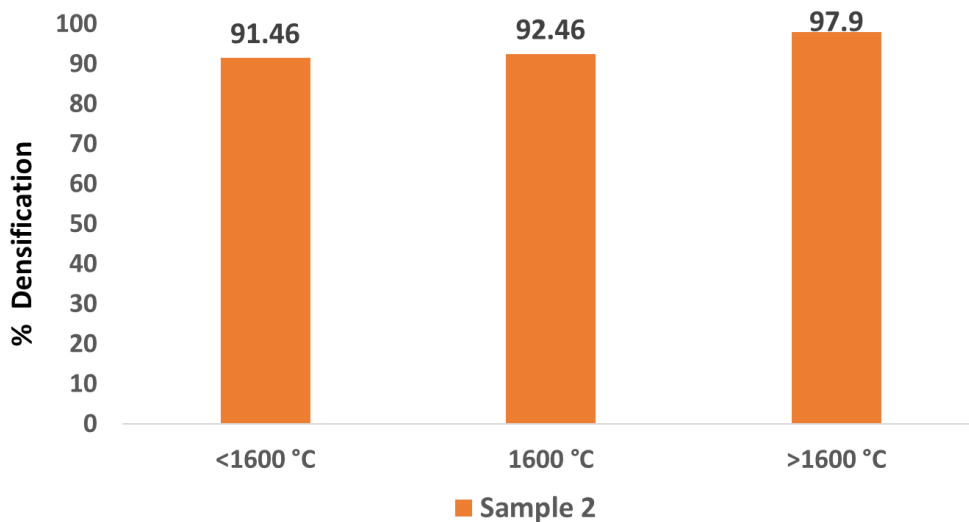


Figure 26: Densification values of sintered sample 2

Figure 28 shows densification of the alumina + TiO<sub>2</sub> + MgO (sample 3) with temperature. It can be seen that percentage densification obtained at temperature <1600 °C is 92.88 and increased to 98.9 percent by increasing the sintering temperature.

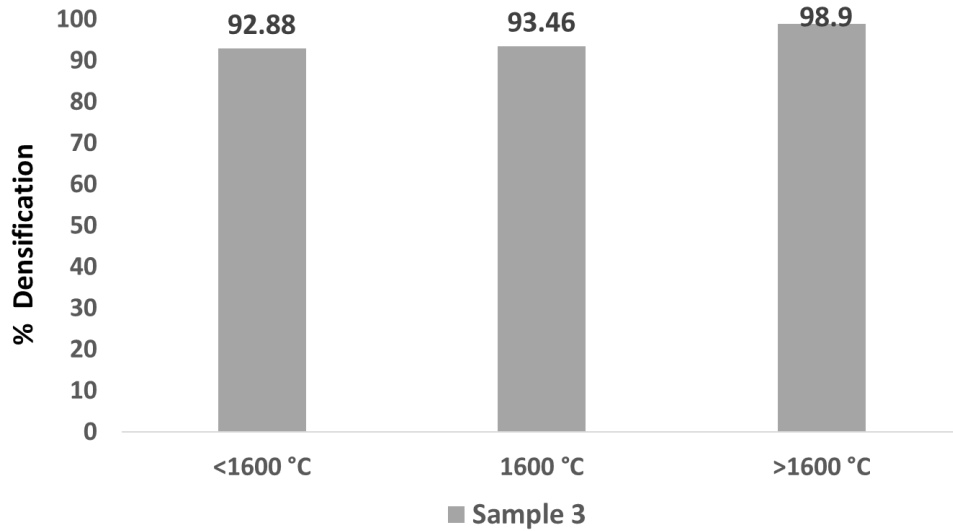


Figure 27: Densification values of sintered sample 3

Figure 29 below shows densification of the alumina + TiO<sub>2</sub> + SiO<sub>2</sub> (sample 4) with temperature. It can be seen that percentage densification obtained at temperature 1575°C is 92.25% and increased to 99.9 percent by increasing the sintering temperature.

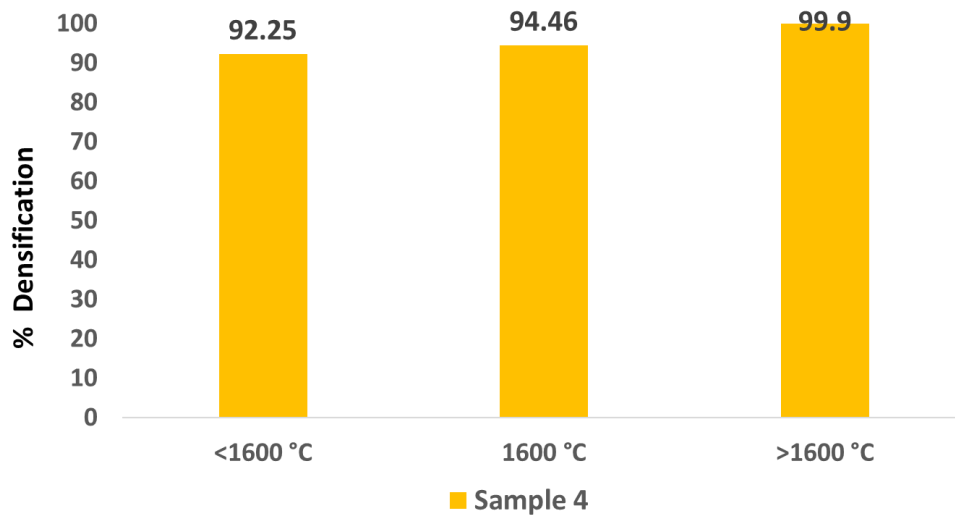


Figure 28 : Densification values of sintered sample 4

All the four bar graphs shown above indicate that with increasing temperature, porosity of all the four samples decreased and densification increased. It means that sintering done at >1600 °C is near to ideal to fabricate ceramic tiles for final armour.

### **3.3.2.2 Effect of additives on experimentally calculated density**

By adding the additives in all synthesized samples, it was observed that densification was increased as compared to pure alumina. Maximum densification was observed in sample 3 at the temperature  $<1600\text{ }^{\circ}\text{C}$  and for the sample 4 at the temperature  $1600\text{ }^{\circ}\text{C}$  and  $>1600\text{ }^{\circ}\text{C}$ . By adding the additives in all synthesized samples, it was observed that densification was increased as compared to pure alumina. Archimedes principle was used to calculate density and it was observed that density increased as compared to pure alumina.

### **3.3.2.3 Effect of additives on densification**

As densification of the samples increases with the increasing temperature, similarly additives also play very important role in densification of the samples. It can be seen in the bar graph densification of the all-other samples as compared to pure alumina increases which clearly indicates that fillers enhance the densification of the samples. At  $<1600\text{ }^{\circ}\text{C}$ , when the comparison of the bar graphs of all the samples is performed, it is concluded that densification achieved by sample no 3 is better than all because of the controlled grain growth and enhancement densification that occurred due to the addition of additives.



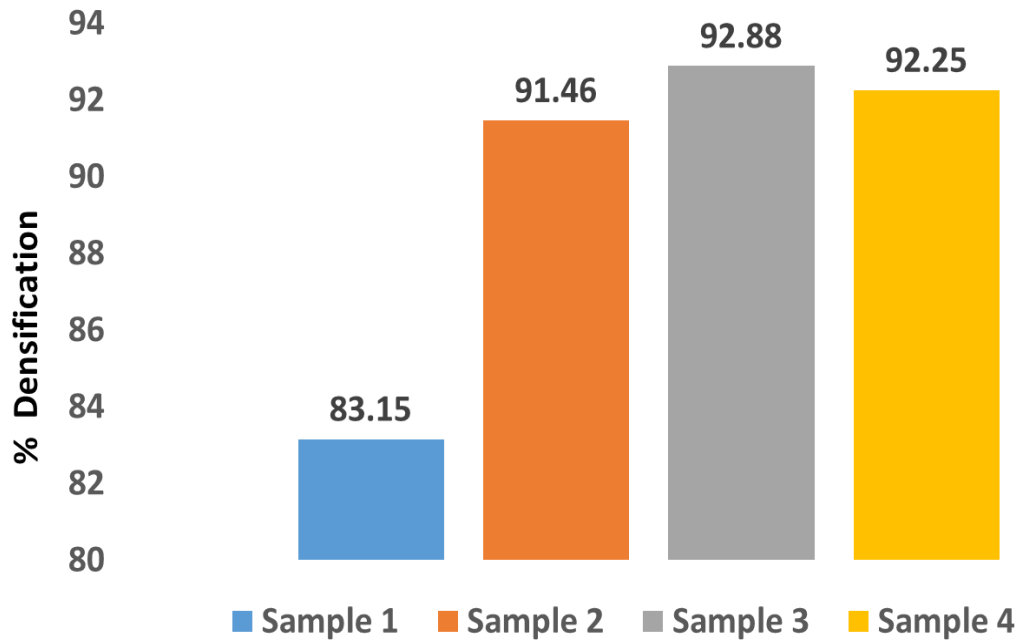


Figure 29: Densification values of sintered samples @<1600 °C

At <1600°C results of densification of all the samples can be seen in bar graph, from which it is concluded that densification achieved by sample no 3 is more than all other samples.

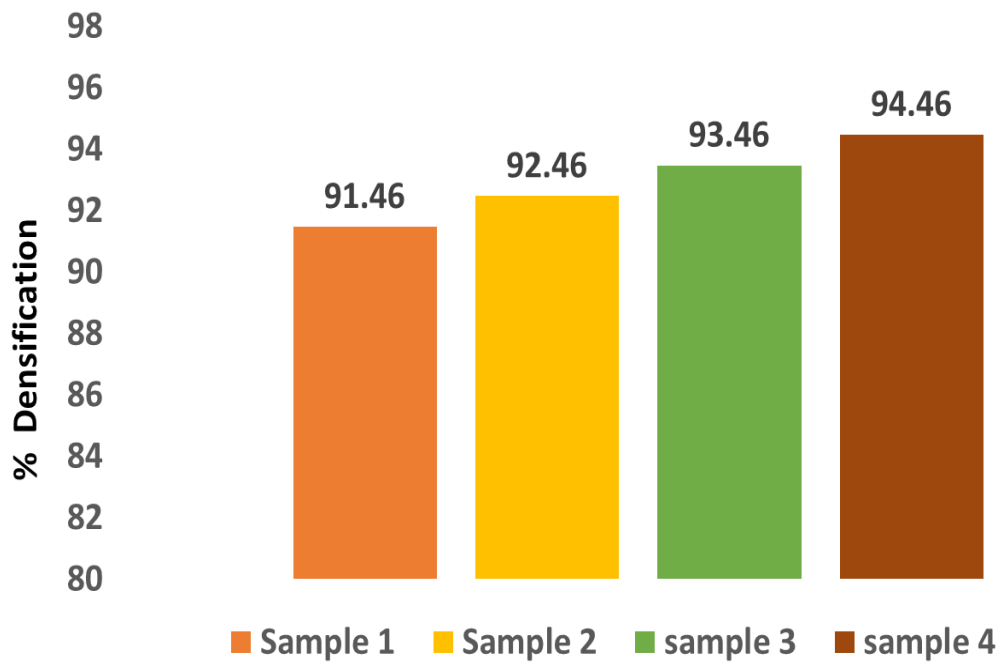


Figure 30: Densification values of sintered samples @1600 °C

At 1600 °C comparison of all the samples is done, and again same increasing trend in densification value is observed.

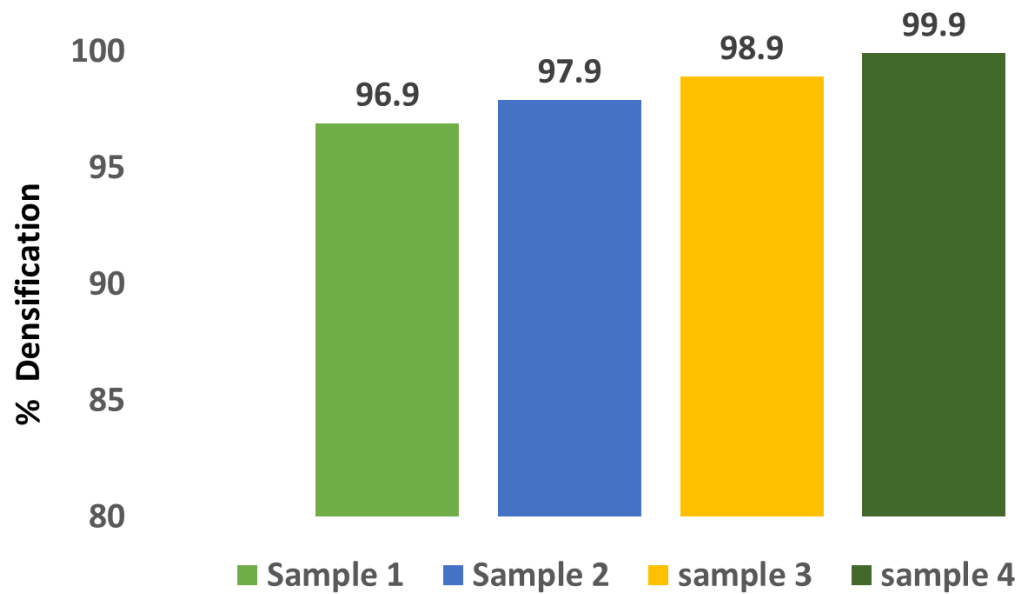


Figure 31: Densification values of sintered samples @>1600°C

Similarly, same trend in densification is observed here at highest temperature.

The densification of the sintered samples can be seen in the table 4.

Table 5: Densification values of sintered samples

<b>Sr.no</b>	<b>Experimentally calculated Density (g/cm<sup>3</sup>)</b>	<b>Densification (%)</b>
<b>EXP # 1 &lt;1600°C</b>		
Sample 1	3.28	83.15
Sample 2	3.61	91.46
Sample 3	3.67	92.88
Sample 4	3.64	92.25
<b>EXP # 2@1600°C</b>		
Sample 1	3.61	91.46
Sample 2	3.76	92.46
Sample 3	3.81	93.46
Sample 4	3.73	94.46
<b>EXP # 3 @&gt;1600°C</b>		
Sample 1	3.83	96.9
Sample 2	3.9	97.9
Sample 3	3.93	98.9
Sample 4	3.88	99.9

As seen from the densification values of the ceramics, sintering aids result in a better densification of Al<sub>2</sub>O<sub>3</sub> samples. The effect of temperature on the densification of the samples can also be seen in the table above. Generally, a rise in densification values can be observed by increasing sintering temperatures. Overall, samples 3 and 4 possess the best densification out of all the samples sintered at high temperatures.

### **3.4 Results of Mechanical Testing**

The samples were subjected to lab based mechanical testing. That included measuring hardness and compressive strength values.

### 3.4.1 Hardness values of fabricated sample

The table below shows the average hardness values of the samples sintered at the different temperatures under the load of  $1\text{kg}_f$  and dwell time was 10 seconds. The hardness values of samples sintered can be seen in the table 6.

Table 6: Hardness values of the fabricated samples

Sr.no	Average Hardness ( $H_v$ )	Average Hardness (GPa)
<b>EXP # 1 @&lt;1600°C</b>		
Sample 1	$1603.75 \pm 65.40$	15.73
Sample 2	$1948.25 \pm 63.91$	19.11
Sample 3	$2027.75 \pm 67.87$	19.89
Sample 4	$1796 \pm 122.01$	17.61
<b>EXP # 2 @1600°C</b>		
Sample 1	$1881.5 \pm 37.16$	18.45
Sample 2	$2119 \pm 63.60$	20.79
Sample 3	$2379.75 \pm 188.35$	23.34
Sample 4	$1849 \pm 128.14$	18.13
<b>EXP # 3 @&gt;1600°C</b>		
Sample 1	$2197 \pm 105.76$	21.55
Sample 2	$2309.5 \pm 102.44$	22.65
Sample 3	$2887 \pm 122.50$	28.31
Sample 4	$1924.5 \pm 43.7$	18.87

The hardness values of all samples can be seen to increase with increasing sintering temperature.

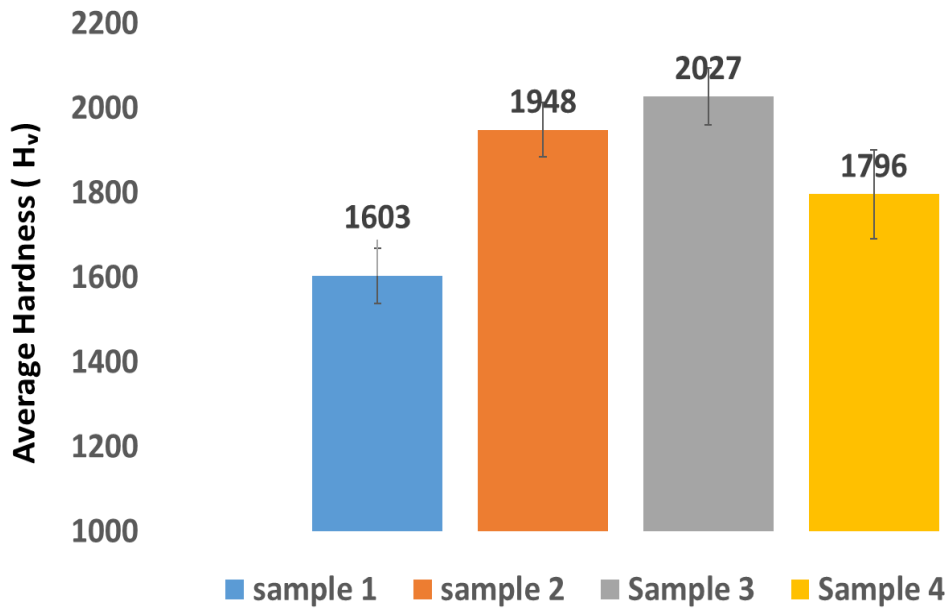


Figure 32: Average hardness values of the samples fabricated @<1600 °C

In above figure 33 it is observed that all the four samples sintered at <1600 °C. Average hardness of the pure alumina was 1603 Hv. But by adding the fillers its hardness increased at the same temperature. Fillers not only fill the gaps of alumina but also provide resistance to crack initiation. Sample no 3 is showing the best results due to the presence of Titania and MgO as explained earlier in SEM images about the role of fillers in ceramic composites.

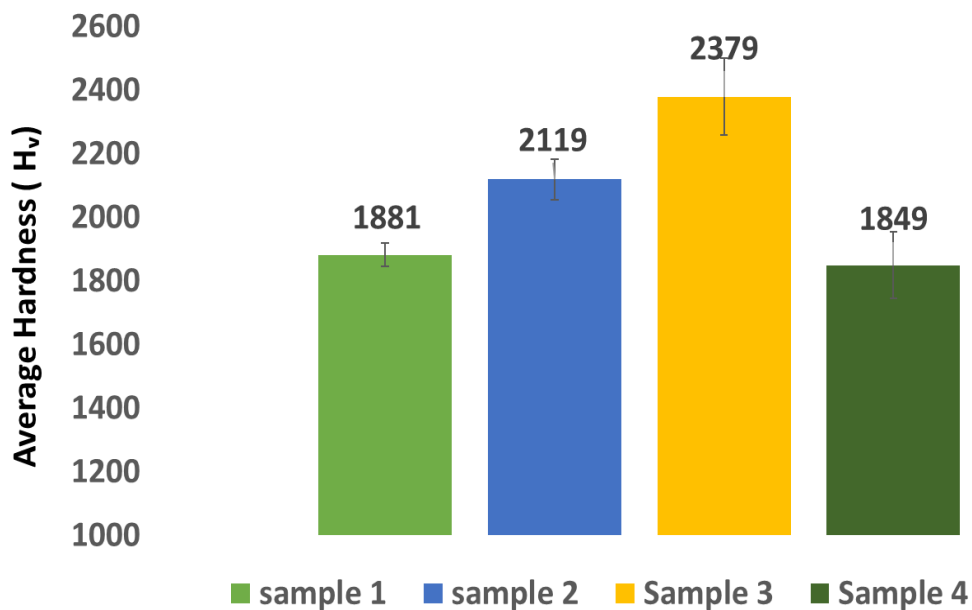


Figure 33: Average hardness values of the samples fabricated @1600 °C

As compared to the samples sintered at temperature  $<1600^{\circ}\text{C}$ , samples sintered at  $1600^{\circ}\text{C}$  have better hardness as depicted in figure 34. The reason behind this may be high sintering temperature which increase the mechanical properties of the alumina based ceramic composites.

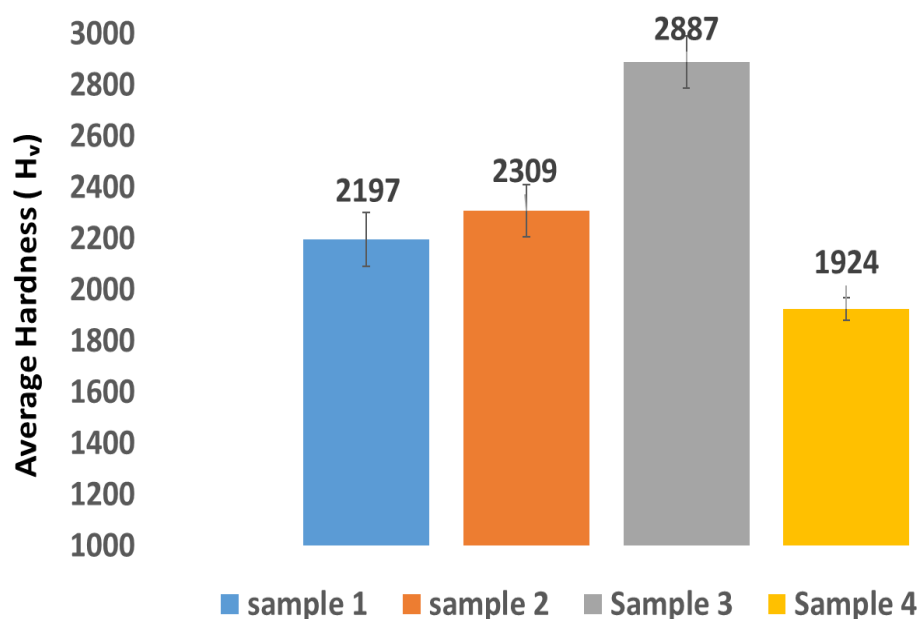


Figure 34: Average hardness values of the samples fabricated @  $>1600^{\circ}\text{C}$

Maximum hardness values are found for sample 3 after being sintered at high temperature that is  $>1600^{\circ}\text{C}$  as shown in figure 35. Sample 4 has lower hardness value due to the presence of silica and silica has glassy appearance which can be seen in SEM image as well. Further increase in sintering temperature increases the sintering capability which is the main reason of getting better mechanical properties. However further increase in temperature, grain growth leads to reduction of flexural strength. On the basis of hardness values and densification results, samples sintered at  $>1600^{\circ}\text{C}$  were chosen for compression testing.

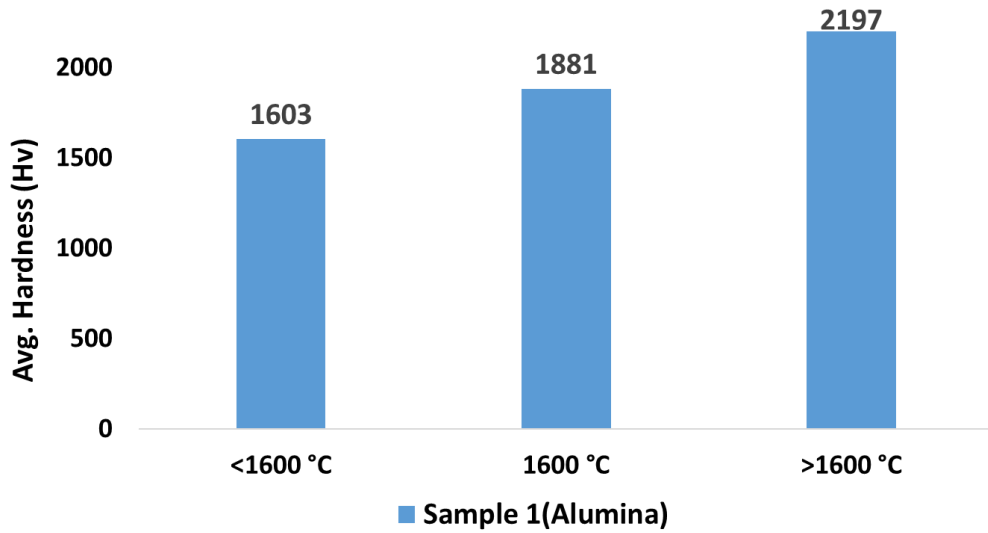


Figure 35: Average hardness values of sample 1

Figure 36 is the comparison of hardness values of the same sample 1 at different temperature. Results show that in sintering temperature increases the sintering capability which is the main reason of getting better mechanical properties. Similar behavior is observed for the sample no. 2,3 and 4 depicted in figure 37,38 and 39 respectively.

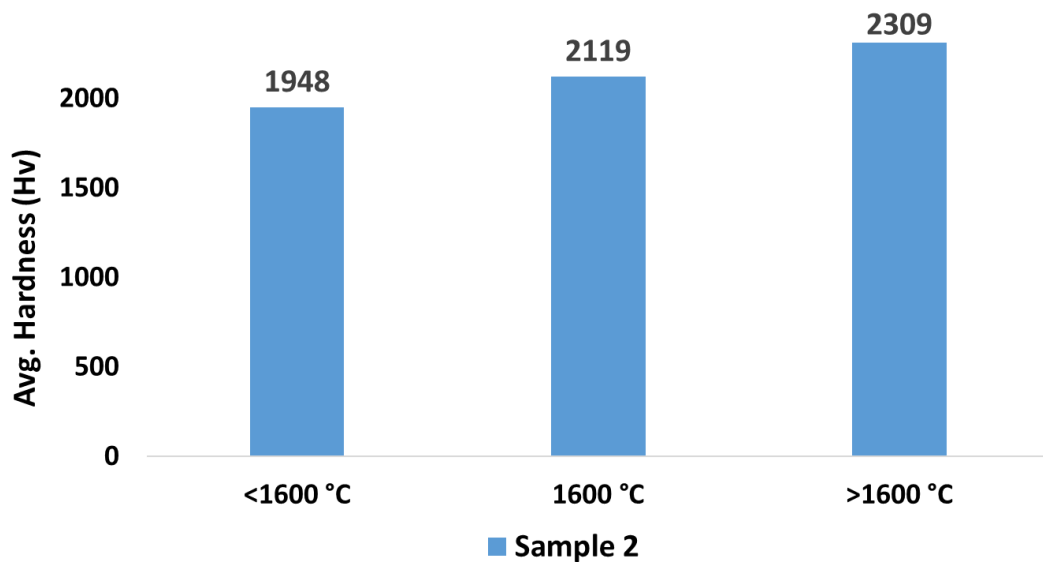


Figure 36: Average hardness values of sample 2

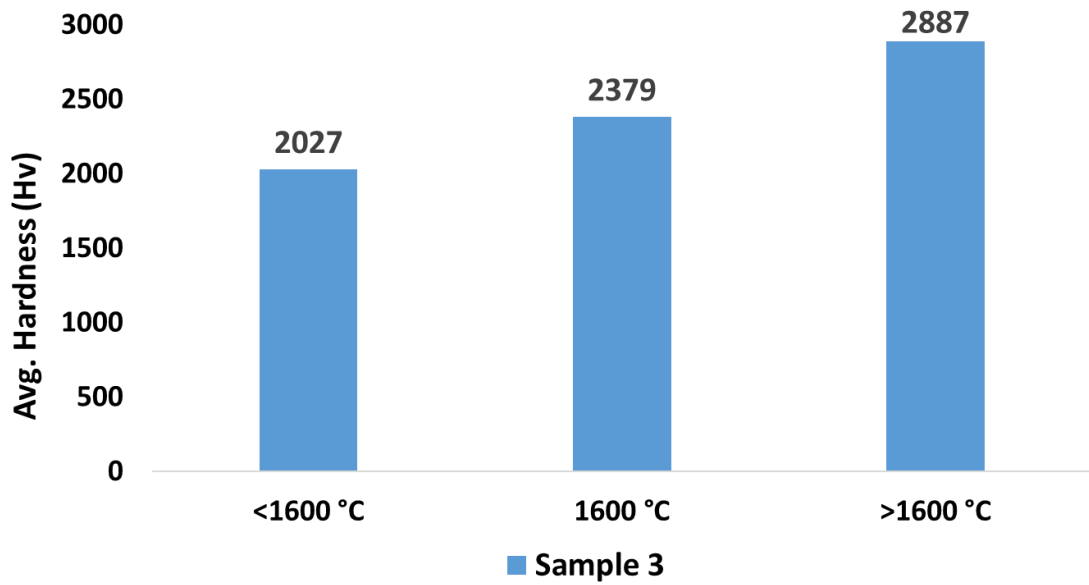


Figure 37: Average hardness values of sample 3

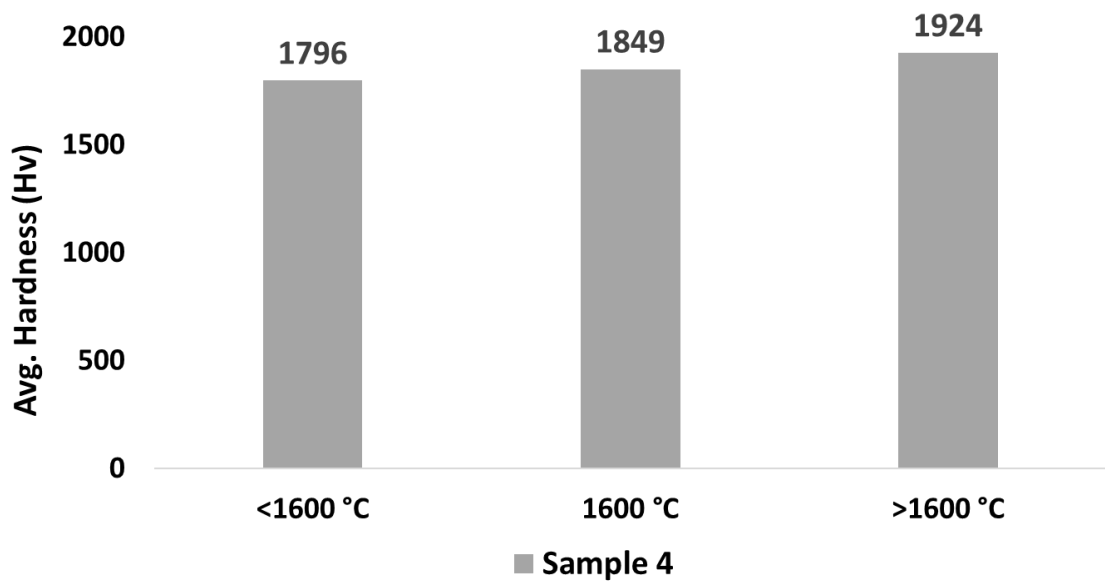


Figure 38 : Average hardness values of sample 4

### 3.4.2 Compressive strength and Young's Modulus of fabricated samples

The values of compressive strengths and young's modulus are as follow in table 7.



Table 7 : Compressive strength values of the samples fabricated

Sr. No	Compressive Strength (MPa)	Young's Modulus (GPa)
Sample 1	2056 ± 20.14	220 ± 2.1
Sample 2	2280 ± 25.24	255 ± 2.3
Sample 3	2821 ± 21.52	320 ± 3.2
Sample 4	1764 ± 23.25	190 ± 1.8

Compressive strength of sample 3 again has highest value as compared to other samples. Similarly, young's modulus of sample 3 is higher in comparison of all the samples.

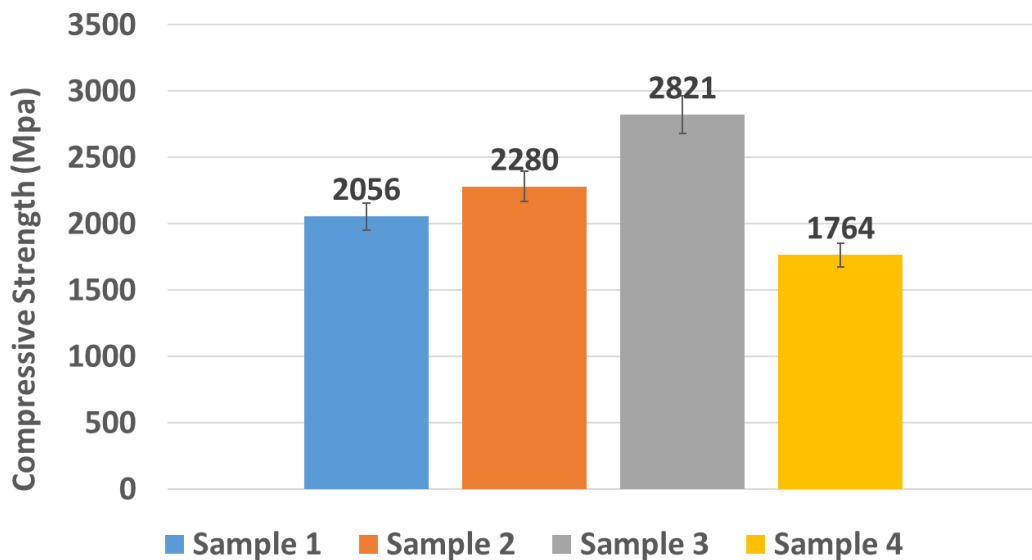


Figure 39: Compressive Strength of Sintered Samples

Additives increase the mechanical properties like compressive strength and young's modulus as can be seen in the bar graphs. This is again due to controlled grain growth because of the addition of the additives as shown in figure 40 and 41.

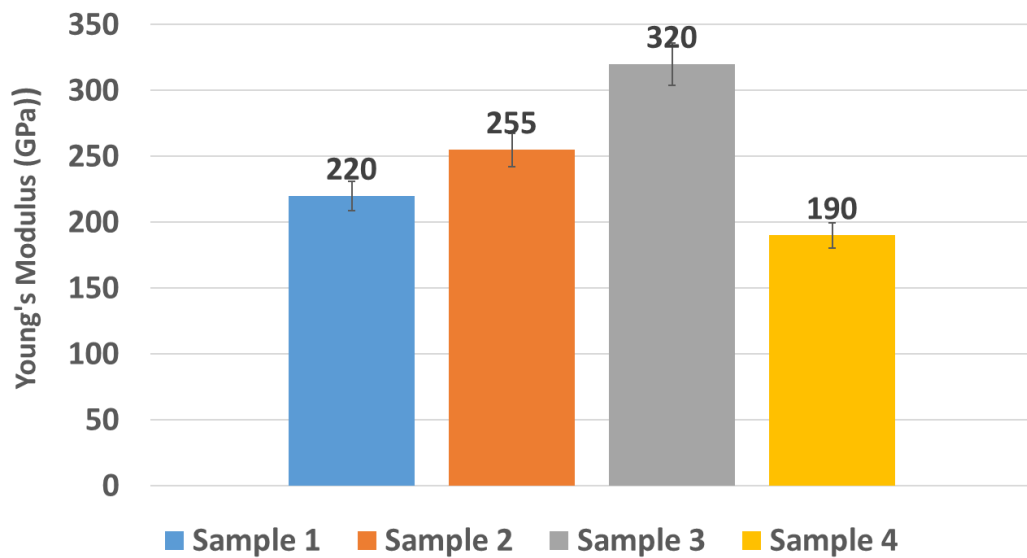


Figure 40 : Young's Modulus of Sintered Samples

By comparing the values of the compressive strength and young's modulus of fabricated samples, sample 3 is showing maximum value. Young modulus is actually the tensile or compressive strength divided by the strain. It means that strain produced in sample 1,2 & 4 is more than the sample 3. To choose the final ceramic composite for ballistic performance based on the different properties, the sample no 3 was selected as the best sample for large scale fabrication.

## Chapter 4: Ballistic testing

An important part is played by ballistic experimentation to understand primary and perilous major issues pertaining to mechanics of armour, its composition and its applications. Excessive safety procedures are required to conduct experimentation of high velocity projectile's impact on target.

Description of experimentation has been given below. These ballistic experimentations and tests are usually performed in defense departments authorized by the government for guaranteeing the safety of observer, researcher and other individuals. Hence, standards and codes of ballistic testing must be implemented for precise results and safety.

To depict performance of a ballistic material,  $V_0$  and  $V_{50}$  are the two typically applied experimental procedures. The velocity at which ballistic projectiles of known shape and mass are stopped and defeated by the target is known as  $V_0$  while the velocity at which 50% or half of the fired rounds of projectile having known mass and geometry pass through the target is called  $V_{50}$ .

Material's ballistic limit is the velocity at which a certain projection when fired at a specific angle, penetrates the material. Ballistic limit technique is also used in experimentation. Another method generally used to assess protection provided by material in reenactments is decreasing kinetic energy of projectile upon impact with the target.

During research on ballistic performance, it is rudimentary to determine performance of protection by backing with dense deposit of clay for finding the depth of projectile by measuring impression made in clay. An armour plate of predefined thickness is mounted on a stand in desired spot and distance from position of gun or launcher in typical ballistic experimentation. For acquiring required data from experimentation, specialized instruments and equipment are used. Diameter of perforations is also critical parameter in determining the fracture of armour material.

Many scholars have used high speed imaging techniques to study ballistic interactions during last few years which help in capturing critical moments of ballistic proliferation. Digital high speed camera was used by Børvik et al. to visualize projectile's infiltration process [3].

The image converter camera delivers very fast shutter speeds, whereas the Charged Coupled Device camera provides digital images instantly after the experimentation. The data collected was used to find velocity.

In ballistic experimentation, following two scenarios can occur either projectile hits the armor and disintegrates into various fragments or the projectile penetrates the armor material. The four phases of bullet velocity that have been described by different researchers are as under:

1. Free flight of projectile
2. Interaction with target on impact
3. Perforation into the target
4. Subsequent flight after penetration

#### **4.1 Testing Standards**

The Standards and Testing Program is sponsored by the Office of Science and Technology of the National Institute of Justice (NIJ), Office of Justice Programs, U.S. Department of Justice.

Type III hard armour or plate inserts shall be tested in a conditioned state with 7.62 mm FMJ, steel jacketed bullets (U.S. Military designation M80) with a specified mass of 9.6 g (147 gr) and a velocity of  $847 \text{ m/s} \pm 9.1 \text{ m/s}$  ( $2780 \text{ ft/s} \pm 30 \text{ ft/s}$ ).

Type III flexible armour shall be tested in both the "as new" state and the conditioned state with 7.62 mm FMJ, steel jacketed bullets (U.S. Military designation M80) with a specified mass of 9.6 g (147 gr) and a velocity of  $847 \text{ m/s} \pm 9.1 \text{ m/s}$  ( $2780 \text{ ft/s} \pm 30 \text{ ft/s}$ ).

For a Type III hard armour or plate insert that will be tested as an in-conjunction design, the flexible armour shall be tested in accordance with this standard and found compliant as a stand- alone armour at its specified threat level. The combination of the flexible armour and hard armour/plate shall then be tested as a system and found to provide protection at the system's specified threat level. NIJ approved hard armours and plate inserts must be clearly labeled as providing ballistic protection only when worn in conjunction with the NIJ-approved flexible armour system with which they were tested.

## 4.2 Experimental Setup

Experiments of ballistic testing were performed to determine the response of Ballistic armour plate. The Ballistic armour plate is normally used for the protection of security personals and in modern era for the protection of security vehicles along with ballistic steel to give protection against threats.

The Ballistic armour is a combination of hexagonal tiles mounted on top of UHMWPE panels to provide the best combination of the protection and weight. Frontal ceramic not only break the sharpness of the incoming projectile but also reduce the speed of the projectile due to which it is stopped in backing plate and cause a trauma in backing plate. The ballistic armour plates were impacted by 7.62 x 51mm lead core bullet. The bullet has an outer Brass jacket and inner lead core as shown in Figure 42.



Figure 41: 7.62 mm armour Piercing Bullet

The velocity of projectile was measured using a chronograph, which was placed 1 m away from the rifle in direction of target. The bullets were fired on each of the different Ballistic armour having different thickness of ceramic tiles to determine ballistic response. The projectile velocity was found between 860~920 m/s. All experiments were recorded using a High-Speed Camera manufactured by Vision Research, United States. High speed camera captured the actual interaction of the bullets and the ceramic tiles. As fabricated ballistic armour was without splinter foil that keep the ceramic tiles intact with the base plate due to this reason all the tiles flown away when bullet hit the ceramic tile.

#### 4.2.1 Case 1: Ceramic tiles having thickness = 10 mm

In case 1, ballistic response of 10 mm thick ceramic tile was observed. Experimental setup is depicted in figure 43 shown below. It consisted of base ballistic armour, high speed camera, gun and chronograph. The chronograph was placed 1 meter from the gun. Ballistic armour plate was placed 10 meters from the gun as shown below.

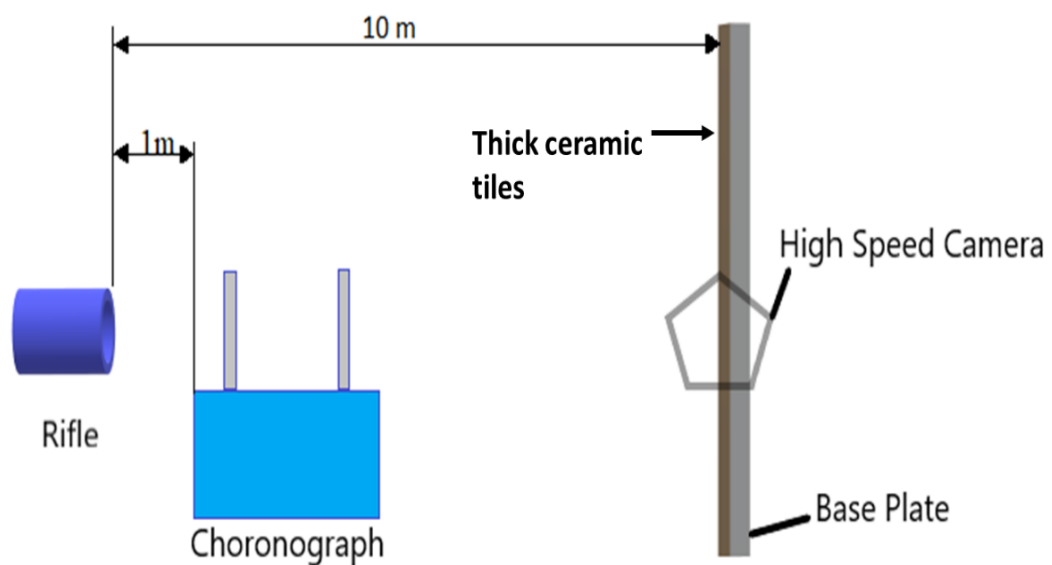


Figure 42: Live firing setup for ceramic tiles having thickness = 10 mm

#### 4.2.2 Case 2: Ceramic tiles having thickness = 5 mm

It consisted of base Ballistic armour, high speed camera, gun and chronograph. The chronograph was placed 1 meter from the gun. Ballistic armour plate was placed 10 meters from the gun as shown below in figure 44.

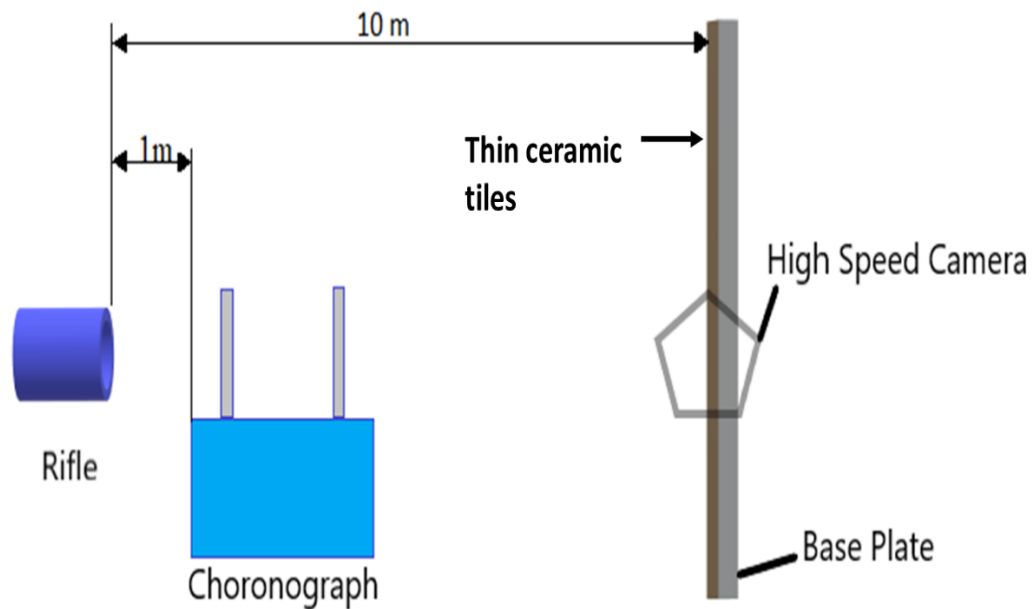


Figure 43: Live firing setup for ceramic tiles having thickness = 5 mm

#### 4.3 Live Ballistic testing of the locally fabricated samples

The greatest extent of indentation in the backing material caused by a non-perforating impact on the armour. The backfixture. One plane contains the reference point on the original (pretest) backing material surface that is co-linear with the bullet line of flight.

If armour were not present, the bullet face signature BFS is the perpendicular distance between two planes, both of which are parallel to the front surface of the backing material would strike this point.)

The other plane contains the point that represents the deepest indentation in the backing material. Depending on bullet–armour backing material interactions, the two points that define the locations of the measurement planes may not be co-linear with the bullet line of flight. Examples of how BFS is measured are shown in the figure 45.

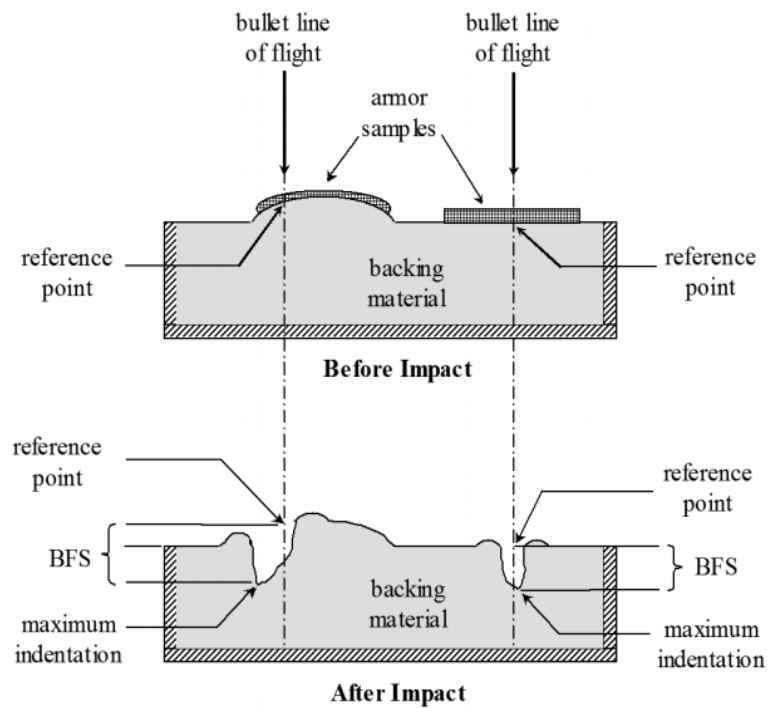


Figure 44 : Examples of BFS systems

The ballistic layer was fixed in a metal structure, clamped between the two ends that were screwed together. This can be seen in the figure 46, 47 and 48.





Figure 45 : Fixation of ballistic panel for testing



Figure 46 : Ballistic panel after first shot



Figure 47 : Ballistic panel after second shot

As seen in the figures above, two types of tiles were used for ballistic tests. One having an overall thickness of 5mm and the others with 10mm. As seen from these images, the bullet was able to penetrate a little bit on the front side of the backing plate having a tile thickness 5mm, while almost no penetration was observed on the front side of the backing plate for the tiles having thickness of 10mm. As ceramic tiles were without splinter foil or honey comb structure that keep the tiles intact due to this reason tiles were flown away in both the cases. The backside of the panel, after test, can be observed to study the depth of penetration of the bullet. This can be seen in the images 49 and 50.

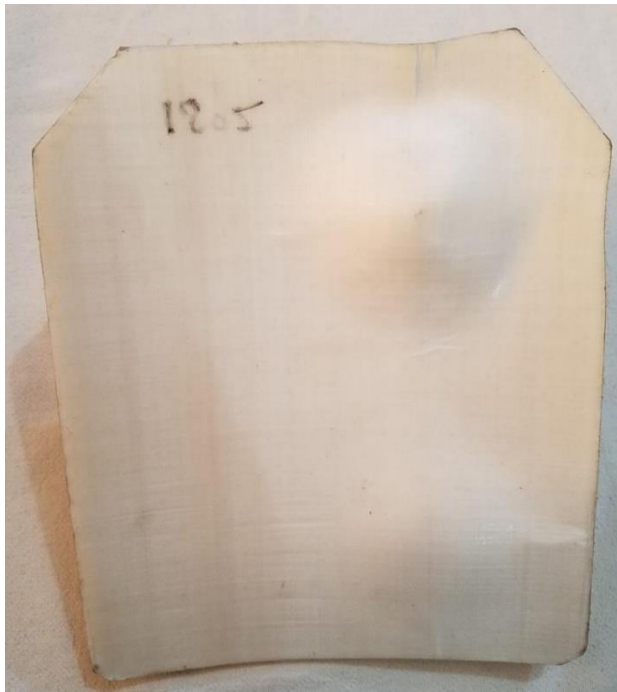


Figure 48: Back side of the panel after ballistic test



Figure 49: Side view of the panel showing trauma after testing

The value of trauma on the back side of the panel after ballistic test was measured with the help a vernier caliper. This value corresponds to the protrusion generated when a bullet hits the panel at high speed. Both types of ceramic tiles were able to resist the impacts of the bullets fired.

However, the values of traumas in both cases were seen to be different. The bullet impacting the ceramic tiles of thickness of 5mm were able to generate a protrusion of roughly 2cm at the back.

However, a much lower value of protrusion, nearly 1cm was measured for the bullet impacting 10mm thick ceramic tiles. It is interesting to note that the ceramic tiles tested were completely bare, with the protection system consisting of only the tiles mounted on to a UHMWPE panel. Practically, a proper armour design consists of layer(s) of Kevlar reinforced epoxy sandwiched in between in order to provide a higher protection by a combination of different layers.

#### 4.4 Comparison with literature

The comparison of different parameters of ballistic sample of this research work is done with literature and found that all the properties are under required conditions as shown in the following table.

Table 8: Comparison of literature with current research work

<b>Properties</b>	<b>Literature value [42]</b>	<b>This research work</b>
Bulk density (g/cm <sup>3</sup> )	>3.85	3.93
Hardness (H <sub>v</sub> )	>1600	2887
Young Modulus (GPa)	>330	320
Trauma (cm)	<4.4	1 (for Type1) 2 (for Type 2)

From above table, it is clear depicted that the values of bulk density, Hardness value, Young Modulus and Trauma values are successfully achieved.

## Conclusion

Light weight ballistic armour is being employed for the safety of military and security personnel. This lightweight armour is composed of composite sheets assembled together to provide maximum protection against high velocity moving objects/projectiles. In Pakistan, HIT, Heavy Industries Taxila is the leading consumer and supplier for this armour equipment. Modern lightweight armour is attached to armoured vehicles and is also worn in bullet-proof vests for protection to military and security personnel throughout the country. When attached to vehicles, they provide protection from gun fire and projectiles. The challenge is to offer the highest level of protection without increasing weight. In this research work, the researcher has successfully analyzed and characterized the genuine sample of imported ballistic armour. Then High density  $\text{Al}_2\text{O}_3$  tiles were successfully fabricated and optimized on a lab scale for strength and performance by using different composition of  $\text{MgO}$ ,  $\text{TiO}_2$  and  $\text{SiO}_2$ . High density  $\text{Al}_2\text{O}_3$  ceramics were optimized, with respect to their microstructure, densification and mechanical properties, on a lab scale first before the fabrication of ceramic tiles. After ceramic samples preparation, cladding of  $\text{Al}_2\text{O}_3$  sintered compacts with Aramid fibers and high-density polyethylene was performed for the local fabrication of composite armour. An armour system for bulletproof vests, consisting of multiple layers has been fabricated. Then, these composite armours were subjected for field testing. Field testing of bare ceramic tiles on top of UHMWPE panel was carried out as per standard procedures. Bare ceramic tiles successfully stopped incoming projectiles by crushing the bullet. Soft armour that is used as a backing plate absorbed the remaining kinetic energy which developed trauma in acceptable range.

## References

- [1] B. P. Kneubuehl, "General wound ballistics," in *Wound ballistics*, Springer, (2011), pp. 87–161.
- [2] N. I. J. Standard, "0108.01: Ballistic Resistant Protective materials," *US Dep. Justice. Natl. Inst. Justice*, (1985).
- [3] T. Børvik, M. Langseth, O. S. Hopperstad, and K. A. Malo, "Ballistic penetration of steel plates," *Int. J. Impact Eng.*, vol. 22, no. 9–10, pp. 855–886, (1999).
- [4] D. Carlucci, *Ballistics: theory and design of guns and ammunition*. (2007). [Online]. Available: <https://www.taylorfrancis.com/books/mono/10.1201/9781420066197/ballistic-s-donald-carlucci>
- [5] C.-K. Chu and Y.-L. Chen, "Ballistic-proof effects of various woven constructions," *Fibres Text. East. Eur.*, (2010).
- [6] D. E. Carlucci, "Ballistics : Theory and Design of Guns and Ammunition," Dec. (2007), doi: 10.1201/9781420066197.
- [7] T. Huaixiang, "Costume Craftwork on a Budget : Clothing, 3-D Makeup, Wigs, Millinery & Accessories," *Costume Craftwork a Budg.*, Nov. (2012), doi: 10.4324/9780080546001.
- [8] U. S. Congress, "Advanced materials by design," *Washington, DC US Gov. Print. Off.*, (1988).
- [9] P. Karandikar, G. Evans, S. W.-... in C. A. IV, and U. (2009), "A review of ceramics for armor applications".
- [10] R. M. Coupland, M. A. Rothschild, and M. J. Thali, "Wound Ballistics," (2011), doi: 10.1007/978-3-642-20356-5.
- [11] M. Specification, "Armor Plate, Steel, Wrought, Homogeneous (for use in Combat-vehicles and for Ammunition Testing), MIL-A-12560H," (1984).
- [12] W. A. Gooch, D. D. Showalter, M. S. Burkins, V. Thorn, S. J. Cimpoeru, and R. Barnett, "Ballistic testing of Australian Bisalloy steel for armor applications," (2007).
- [13] A. M. R. T. J. Holmquist, "A Ceramic Armor Material Database,U.S. Army

- Tank Automotive Research, Development and Engineering Center, United States 13754,” (1999).
- [14] R. F. A. and D. S. Thompson, “Aluminum Armor Plate System,” United States Patent 4,469,537,” (1984).
- [15] V. S. G. Murray, M. R. Bailey, and B. G. Spratt, “Depleted uranium: a new battlefield hazard,” *Lancet*, vol. 360, pp. s31–s32, Dec. (2002), doi: 10.1016/S0140-6736(02)11811-3.
- [16] R. L. Cook, “Hard Faced Plastic Armor,” United States Patent 3516898,” (1966).
- [17] J. S. Montgomery and M. G. H. Wells, “Titanium armor applications in combat vehicles,” *JOM* (2001) 534, vol. 53, no. 4, pp. 29–32, 2001, doi: 10.1007/S11837-001-0144-2.
- [18] P. J. Hogg, “Composites in armor,” *Science* (80-. ), vol. 314, no. 5802, pp. 1100–1101, (2006).
- [19] M. I. Khan, “Composite solutions: existing and next generation,” in *Composite Solutions for Ballistics*, Elsevier, (2021), pp. 249–265.
- [20] A. K. Bandaru, V. V Chavan, S. Ahmad, R. Alagirusamy, and N. Bhatnagar, “Ballistic impact response of Kevlar® reinforced thermoplastic composite armors,” *Int. J. Impact Eng.*, vol. 89, pp. 1–13, (2016).
- [21] I. Álvarez, R. Torrecillas, W. Solis, P. Peretyagin, and A. Fernández, “Microstructural design of Al<sub>2</sub>O<sub>3</sub>–SiC nanocomposites by spark plasma sintering,” *Ceram. Int.*, vol. 42, no. 15, pp. 17248–17253, (2016).
- [22] V. Garnier, G. Fantozzi, D. Nguyen, J. Dubois, and G. Thollet, “Influence of SiC whisker morphology and nature of SiC/Al<sub>2</sub>O<sub>3</sub> interface on thermomechanical properties of SiC reinforced Al<sub>2</sub>O<sub>3</sub> composites,” *J. Eur. Ceram. Soc.*, vol. 25, no. 15, pp. 3485–3493, (2005).
- [23] G. Zhan, J. D. Kuntz, R. Duan, and A. K. Mukherjee, “Spark- plasma sintering of silicon carbide whiskers (SiCw) reinforced nanocrystalline alumina,” *J. Am. Ceram. Soc.*, vol. 87, no. 12, pp. 2297–2300, (2004).
- [24] K. Takahashi, M. Yokouchi, S. Lee, and K. Ando, “Crack- healing behavior of Al<sub>2</sub>O<sub>3</sub> toughened by SiC whiskers,” *J. Am. Ceram. Soc.*, vol. 86, no. 12, pp. 2143–2147, (2003).

- [25] C. Liu, J. Sun, F. Gong, and B. Li, "Effects of micro and macro features on the thermal shock resistance of laminated Al<sub>2</sub>O<sub>3</sub>–MgO composites," *Ceram. Int.*, vol. 46, no. 7, pp. 9606–9613, (2020).
- [26] C. W. Park and D. Y. Yoon, "Effects of SiO<sub>2</sub>, CaO<sub>2</sub>, and MgO Additions on the Grain Growth of Alumina," *J. Am. Ceram. Soc.*, vol. 83, no. 10, pp. 2605–2609, Oct. (2000), doi: 10.1111/J.1151-2916.2000.TB01596.X.
- [27] Y. Nie, P. B. Oliete, and R. I. Merino, "Influence of microstructural size on the thermal shock behavior of Al<sub>2</sub>O<sub>3</sub>-Er<sub>3</sub>Al<sub>5</sub>O<sub>12</sub> directionally solidified eutectics," *Scr. Mater.*, vol. 160, pp. 20–24, (2019).
- [28] M. I. K. Collin and D. J. Rowcliffe, "Influence of thermal conductivity and fracture toughness on the thermal shock resistance of alumina—silicon—carbide—whisker composites," *J. Am. Ceram. Soc.*, vol. 84, no. 6, pp. 1334–1340, (2001).
- [29] F. Ye, T. C. Lei, and Y. Zhou, "Interface structure and mechanical properties of Al<sub>2</sub>O<sub>3</sub>–20vol% SiCw ceramic matrix composite," *Mater. Sci. Eng. A*, vol. 281, no. 1–2, pp. 305–309, (2000).
- [30] D.-Y. Lee and D.-H. Yoon, "Properties of alumina matrix composites reinforced with SiC whisker and carbon nanotubes," *Ceram. Int.*, vol. 40, no. 9, pp. 14375–14383, (2014).
- [31] M. Parchovianský *et al.*, "Microstructure and mechanical properties of hot pressed Al<sub>2</sub>O<sub>3</sub>/SiC nanocomposites," *J. Eur. Ceram. Soc.*, vol. 33, no. 12, pp. 2291–2298, (2013).
- [32] P. B. Armor, "Ballistic Resistance of Personal Body Armor NIJ Standard–0101.04," (2008).
- [33] "Nano images perfect focus." <https://www.nanoimages.com/sem-technology-overview/> (accessed Jun. 09, (2022)).
- [34] K. Sunil, I. Johri, C. Gedam, P. Jain, J. Deshpande, and harieeshwar, *Effects of Cold Extrusion on Material Properties*. (2018). doi: 10.13140/RG.2.2.28696.14082.
- [35] J. Kang, "Local Density Parameters with respect to Powder Metal Sintering Process," (2019).
- [36] Z. Zhang, W. Liu, Z. Song, and X. Hu, "Two-Step Chemical Mechanical



- Polishing of Sapphire Substrate,” *J. Electrochem. Soc. - J Electrochem SOC*, vol. 157, Jan. (2010), doi: 10.1149/1.3410116.
- [37] K. C. S. Reddy, K. M. S. Kumar, and L. S. R. Yadav, “Synthesis and characterization of magnesium oxide nanoparticles using combustion method to study the fuel properties,” *Mater. Today Proc.*, vol. 49, pp. 797–800, 2022.
- [38] D. L. Liao and B. Q. Liao, “Shape, size and photocatalytic activity control of TiO<sub>2</sub> nanoparticles with surfactants,” *J. Photochem. Photobiol. A Chem.*, vol. 187, no. 2–3, pp. 363–369, (2007).
- [39] W. Stöber, A. Fink, and E. Bohn, “Controlled growth of monodisperse silica spheres in the micron size range,” *J. Colloid Interface Sci.*, vol. 26, no. 1, pp. 62–69, (1968).
- [40] A. H. Mohamed Ariff, M. A. Mohamad Najib, S. Mohd Tahir, A. As’ Arry, and N. Mazlan, “Effect of sintering temperature on the properties of porous Al<sub>2</sub>O<sub>3</sub>-10 wt% RHA/10 wt% Al composite,” *Adv. Mater. Process. Technol.*, vol. 7, no. 3, pp. 417–428, (2021).
- [41] A. Moradkhani, H. Baharvandi, and A. Naserifar, “Effect of sintering temperature on the grain size and mechanical properties of Al<sub>2</sub>O<sub>3</sub>-SiC Nanocomposites,” *J. Korean Ceram. Soc.*, vol. 56, no. 3, pp. 256–268, (2019).
- [42] China Sancera, “Alumina Ceramic Tiles for Ballistic Insert Plate Nij Level III Stand Alone-Alumina Ceramics-Leading supplier of bulletproof Ceramics: (china-sancera.com)

## Copyright Statement

- Copyright in text of this thesis rests with the student author. Copies (by any process) either in full, or of extracts, may be made only in accordance with instructions given by the author and lodged in the Library of NUST School of Chemical and Materials Engineering (SCME). Details may be obtained by the Librarian. This page must form part of any such copies made. Further copies (by any process) may not be made without the permission (in writing) of the author.
- The ownership of any intellectual property rights which may be described in this thesis is vested in NUST School of Chemical and Materials Engineering, subject to any prior agreement to the contrary, and may not be made available for use by third parties without the written permission of the SCME, which will prescribe the terms and conditions of any such agreement.
- Further information on the conditions under which disclosures and exploitation may take place is available from the Library of NUST School of Chemical and Materials Engineering, Islamabad.